AD-A255 703

92-24977

1. Report No. ATC-184	2. Government Accession No. DOT/FAA/NR-91/10	3. Recipient's Catalog No.

4. Title and Subtitle Birds Mimicking Microbursts on 2 June 1990 in Orlando, Florida	5. Report Date 10 July 1992
	6. Performing Organization Code

7. Author(s) M.A. Isaminger	8. Performing Organization Report No. ATC-184

9. Performing Organization Name and Address Lincoln Laboratory, MIT P.O. Box 73 Lexington, MA 02173-9108	10. Work Unit No. (TRAIS)
	11. Contract or Grant No. DTFA-01-89-Z-02033

12. Sponsoring Agency Name and Address Department of Transportation Federal Aviation Administration Systems Research and Development Service Washington, DC 20591	13. Type of Report and Period Covered Project Report
	14. Sponsoring Agency Code

15. Supplementary Notes

16. Abstract

During 1990 and 1991, the Terminal Doppler Weather Radar (TDWR) testbed collected Doppler radar measurements in Orlando, Florida in support of the TDWR Project. The main focus of the project is to develop algorithms that automatically detect wind shears such as microbursts and gust fronts. While the primary goal of the TDWR is to detect scattering from raindrops, the sensitivity of the system allows for the detection of biological echoes as well. Previous research has shown that under certain conditions the scattering from birds and insects will lead to divergent signatures that mimic microbursts. This type of pattern has been documented in Alabama (Rinehart, 1986), Illinois (Larkin and Quine, 1989), and Missouri (Evans, 1990). In the Alabama and Illinois events, a divergent pattern similar to a microburst was produced when a large number of birds departed in the early morning hours from an overnight roosting site.

On 2 June 1990 in Orlando, Florida, there were 11 surface divergent signatures similar to microbursts detected by the TDWR testbed radar. The maximum differential velocity of these events ranged from 11 to 36 m/s, while the maximum reflectivity varied from 0 to 44 dBz. There was light rain in the area and low-reflectivity returns aloft; however, the reflectivity was more like low-reflectivity microbursts in Denver than high-reflectivity microbursts that generally are observed in Orlando. These divergences were not detected by the microburst algorithm since the TDWR site adaptation parameters have been adjusted to avoid issuing alarms for signatures such as those on 2 June. Detailed investigation was conducted of two events to verify that these were not actual microbursts.

Single Doppler radar features identified in earlier observations of divergence signatures caused by birds in Alabama and Missouri, as well as features suggested by NEXRAD researchers, were considered. The results of the radar data analysis could not unequivocally determine that birds caused the divergent signatures. A microburst prediction model developed by Wolfson was applied to the data using sounding results from Cape Canaveral, Florida to determine whether the apparent velocities were consistent with current theories of microburst generation. This model analysis clearly indicates a nonweather-related cause for the divergent signatures observed on 2 June. We conclude from the microburst prediction analysis and certain oddities in the divergence radar signatures that birds probably accounted for these divergences.

17. Key Words birdburst stipple reflectivity asymmetry dry microburst outflow prediction forcing mechanisms	18. Distribution Statement This document is available to the public through the National Technical Information Service, Springfield, VA 22161.

19. Security Classif. (of this report) Unclassified	20. Security Classif. (of this page) Unclassified	21. No. of Pages 78	22. Price

FORM DOT F 1700.7 (8-72)   Reproduction of completed page authorized

ABSTRACT

During 1990 and 1991, the Terminal Doppler Weather Radar (TDWR) testbed collected Doppler radar measurements in Orlando, Florida in support of the TDWR Project. The main focus of the project is to develop algorithms which automatically detect wind shears such as microbursts and gust fronts. While the primary goal of the TDWR is to detect scattering from raindrops, the sensitivity of the system allows for the detection of biological echoes as well. Previous research has shown that under certain conditions the scattering from birds and insects will lead to divergent signatures which mimic microbursts. This type of pattern has been documented in Alabama (Rinehart, 1986), Illinois (Larkin and Quine, 1989) and Missouri (Evans, 1990). In the Alabama and Illinois events, a divergent pattern similar to a microburst was produced when a large number of birds departed in the early morning hours from an overnight roosting site.

On 2 June 1990 in Orlando, Florida there were 11 surface divergent signatures similar to microbursts detected by the TDWR testbed radar. The maximum differential velocity of these events ranged from 11 to 36 m/s, while the maximum reflectivity varied from 0 to 44 dBz. There was light rain in the area and low−reflectivity returns aloft; however, the reflectivity was more like low−reflectivity microbursts in Denver than high−reflectivity microbursts that generally are observed in Orlando. These divergences were not detected by the microburst algorithm since the TDWR site adaptation parameters have been adjusted to avoid issuing alarms for signatures such as occurred on 2 June. Detailed investigation was conducted of two events to verify that these were not actual microbursts.

Single Doppler radar features identified in earlier observations of divergence signatures caused by birds in Alabama and Missouri, as well as features suggested by NEXRAD researchers, were considered. The results of the radar data analysis could not unequivocally determine that birds caused the divergent signatures. A microburst prediction model developed by Wolfson was applied to the data using sounding results from Cape Canaveral, Florida to determine whether the apparent velocities were consistent with current theories of microburst generation. This model analysis clearly indicates a non−weather−related cause for the divergent signatures observed on 2 June. We conclude from the microburst prediction analysis and certain oddities in the divergence radar signatures that birds probably accounted for these divergences.

ACKNOWLEDGMENTS

TABLE OF CONTENTS

LIST OF ILLUSTRATIONS

LIST OF ILLUSTRATIONS
(CONTINUED)

LIST OF TABLES

1. INTRODUCTION

The Terminal Doppler Weather Radar (TDWR) testbed collected weather data on thunderstorms in Orlando, Florida, from 1990 through 1992 in support of the TDWR program. All of the microbursts recorded in Orlando, with the possible exception of the events from 2 June 1990, had a maximum reflectivity of 35 dBz or greater. This was expected based on the moisture regime in the area. In order for low−reflectivity microbursts to develop generally requires 1) a deep, dry sub−cloud layer with a dew point depression below cloud base > 30° C; 2) a temperature lapse rate > 8.5° C/km below 500 mb; 3) a moist layer around 500 mb; and 4) a temperature/dew point spread at the surface > 16.7° C (Wakimoto, 1985 and Caracena and Flueck, 1988). These characteristics are commonly associated with atmospheric soundings from low−reflectivity microburst days in the High Plains region such as Denver, Colorado.

On 2 June 1990 in Orlando, there were 11 low−reflectivity surface divergent signatures similar to microbursts detected by the radar. In this report, two of the strongest divergences will be analyzed to determine if they were caused by birds or weather. Both events were accompanied by a low−reflectivity echo above the surface. The fact that there was weather nearby made their classification more difficult. The primary method of analysis will be single−Doppler radar measurements of the radial velocity, reflectivity and spectral width profile of each event. In addition, a morning sounding containing thermodynamic and wind data from Cape Canaveral, Florida, will be used to 1) characterize the pre−storm atmosphere and 2) determine the variables required to predict the maximum outflow velocities on this day (Wolfson, 1990). The basis for the latter analysis is to determine if an outflow would be possible on this day based on the maximum echo reflectivity and atmospheric characteristics.

The report is divided into the following sections. Section 2. describes some of the characteristics of bird signatures with radar data. This includes a discussion of several diagnostic variables, from a study by Larkin and Quine, which were used to distinguish bird echoes from weather echoes. The radar characteristics of the eleven Orlando low−reflectivity events are presented in Section 3., while Section 4. describes a more detailed analysis of two of the divergences. Section 5. presents a comparison of reflectivity stipple between birds, weather and the two divergences from 2 June. In Section 6., the reflectivity and velocity features aloft associated with the divergences are discussed. The validity of the reflectivity measurements are reported in Section 7. The atmospheric characteristics and predicted outflow velocities are described in Section 8. Potential microburst forcing mechanisms are detailed in Section 9. Section 10. summarizes the key findings, while Section 11. provides a conclusion of whether the events were low−reflectivity microbursts or birds. Section 12. contains a description of future work involving bird measurements with radar in central Florida.

1

2. CHARACTERISTICS OF BIRDBURSTS

While the primary scatterer detected with a Doppler weather radar is raindrops, the sensitivity of the system allows for the detection of biological echoes as well. Under certain conditions the scattering from birds and insects will lead to divergent signatures which mimic microbursts. The most well documented cause for this type of pattern is when a large number of birds depart in the early morning hours from an overnight roosting site. The divergent signature which may result has been called a birdburst. In Kansas City, Missouri, microburst false alarms were generated by both birds and insects (Evans, 1990).

Recent studies have shown that birds can be a significant hazard to an aircraft. Statistics from the United States Air Force shows they experience approximately 3000 bird strikes each year. In fact, a 1987 crash of a B1−B near La Junta, Colorado, occurred as a result of a bird strike (Scott, 1987). Therefore, it would be fortuitous to develop an automated algorithm which can detect and provide warnings for this phenomena. In this regard a TDWR detection of a birdburst would be indicative of a potential hazard to an aircraft. However, declaring a loss value associated with the event would not be correct. Determining the distinguishing characteristics of birdbursts might provide for an algorithm which can differentiate birdbursts even in the presence of weather.

Table 1. contains the characteristics of birdbursts observed by the TDWR testbed in Huntsville, Alabama (1986), Kansas City, Missouri (1989) and Orlando, Florida (1990−1992). The reason these events were classified as birds was due to the lack of a reflectivity or velocity signature above the surface divergence. In addition, the events in Huntsville and Kansas City were verified by field observations. The maximum radial velocity of the birdbursts varied from 12 to 21 m/s, while the maximum surface reflectivity ranged from 14 to 42 dBz. The highest reflectivity in a bird echo was detected with the 9 December 1991 case in Orlando. The strongest event had a maximum velocity differential of 36 m/s. In terms of size, the largest echo was the Huntsville Birdburst which reached a maximum extent of 20 km^2 at the time of maturity (Rinehart, 1986). The duration of these events varied from 6 to >45 min. Therefore, once the birdburst is in progress, its impact can last as long as the typical microburst. The highest number of birds occurred in the Huntsville event, which also had the longest duration. In terms of times of occurrence, most of the bird events were detected in the early morning hours, typically within 30 minutes of sunrise. This was expected since birds typically roost overnight and depart for feeding sites near sunrise. While birdbursts are most common near sunrise, one event from Kansas City shows they can occur at other times of the day.

While examining the reflectivity and velocity characteristics of previous bird events, one striking feature was the significant variability from case to case. This was not unusual since the reflectivity and velocity of the echo will depend on the type and number of birds. The issue was further complicated when the bird echo was co−located with a weather echo. Nevertheless, there were distinct patterns in some bird echoes which could differentiate them from weather. For example, the reflectivity and velocity profiles of birdbursts may show large variations from

3

Table 1.
Characteristics of Birdbursts from Huntsville (1986),
Kansas City (1989) and Orlando (1990–1992)

Location	Date	Event Time (UT)	Sunrise (UT)	Max Vel (m/s)	Max Delta V (m/s)	Max Refl (dBz)	Duration (min)
Huntsville	29 July	1016	1007	12	24	40	> 45
Kansas City*	15 Aug	1130	1128	21	36	20	> 22
Kansas City	6 Sept	1201	1151	20	32	15	> 20
Kansas City	6 Sept	1150	1151	13	24	14	8
Kansas City	14 Aug	0047	1127	12	17	14	6
Orlando 90	12 Sept	1052	1020	17	28	21	8
Orlando 91	9 Dec	1137	1118	15	27	42	20
Orlando 92	12 Mar	1131	1044	20	28	38	16

one radar range gate to the next which results in a spiky distribution. Figure 1. shows the reflectivity profile along the radial containing the maximum reflectivity for a Kansas City event at 120338 UT on 6 September 1989. The profile is characterized by large reflectivity variations over short intervals. In fact, the maximum and minimum reflectivity are separated by only 0.3 km. A reflectivity and velocity image of this and another Kansas City Birdburst on the same day are shown in Figure 2. One event was located at 26 km and 109° (top two panels) and the other at 13 km and 112° (bottom two panels). Both exhibit the divergent pattern of a microburst with a radial velocity differential of between 20 and 30 m/s. The outline of the divergence region is denoted by the polygon on the reflectivity and velocity images. The maximum surface reflectivity in each case was < 20 dBz. There was a low–reflectivity echo above the surface near each divergence. Due to the close proximity of the weather echo and bird echo, it is hypothesized that the birdbursts were caused by rainshowers which disturbed a local population of birds.

Figure 3. shows the velocity distribution at three times for a birdburst on 12 September 1990 in Orlando. The event was detected at 17 km and 157.5°, which is the same location as event # 3 from 2 June 1990. A field survey after the fact showed the event was located in a grove of orange trees near a lake. There are four distinct characteristics of this divergence which are not indicative of a microburst. For one, the velocities do not generally increase with range but show significant variations from one radar range gate to the next, especially at 105248 and
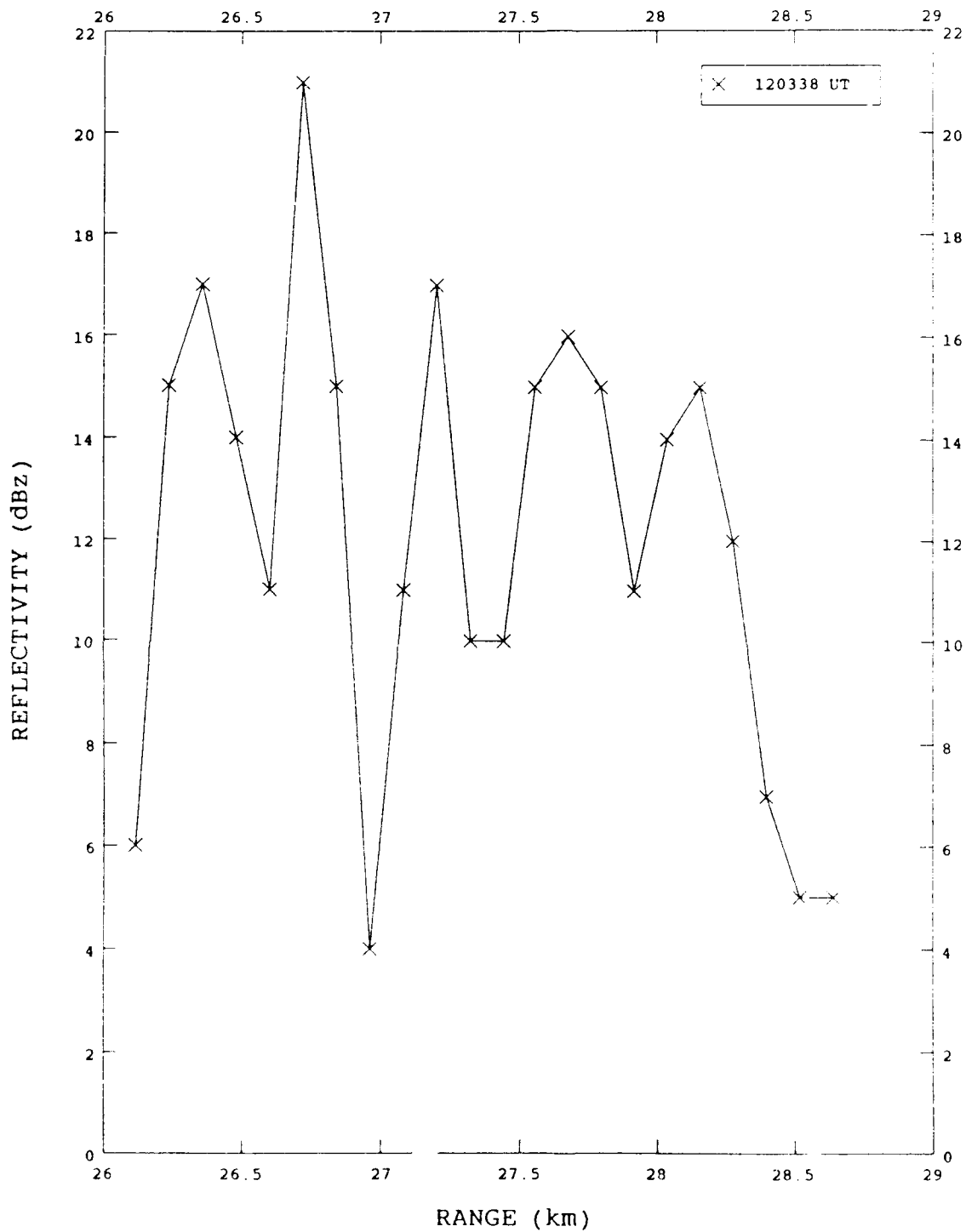
4

Figure 1. Plot of reflectivity vs. range along one radial of a birdburst at 120338 UT on 6 September 1989 in Kansas City, Missouri.
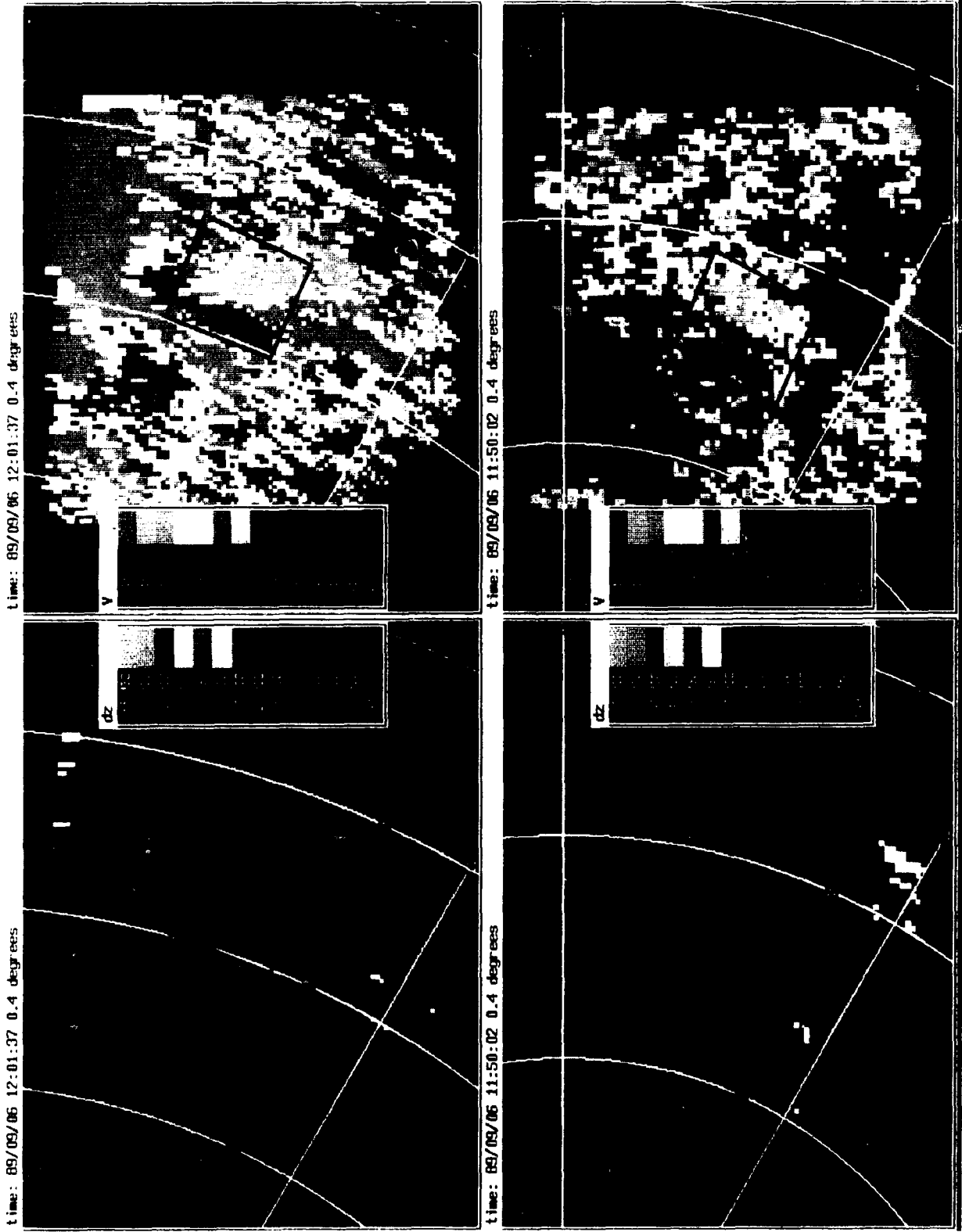
Figure 2. *Reflectivity and velocity images of two birdbursts on 6 September 1989 in Kansas City, Missouri.*
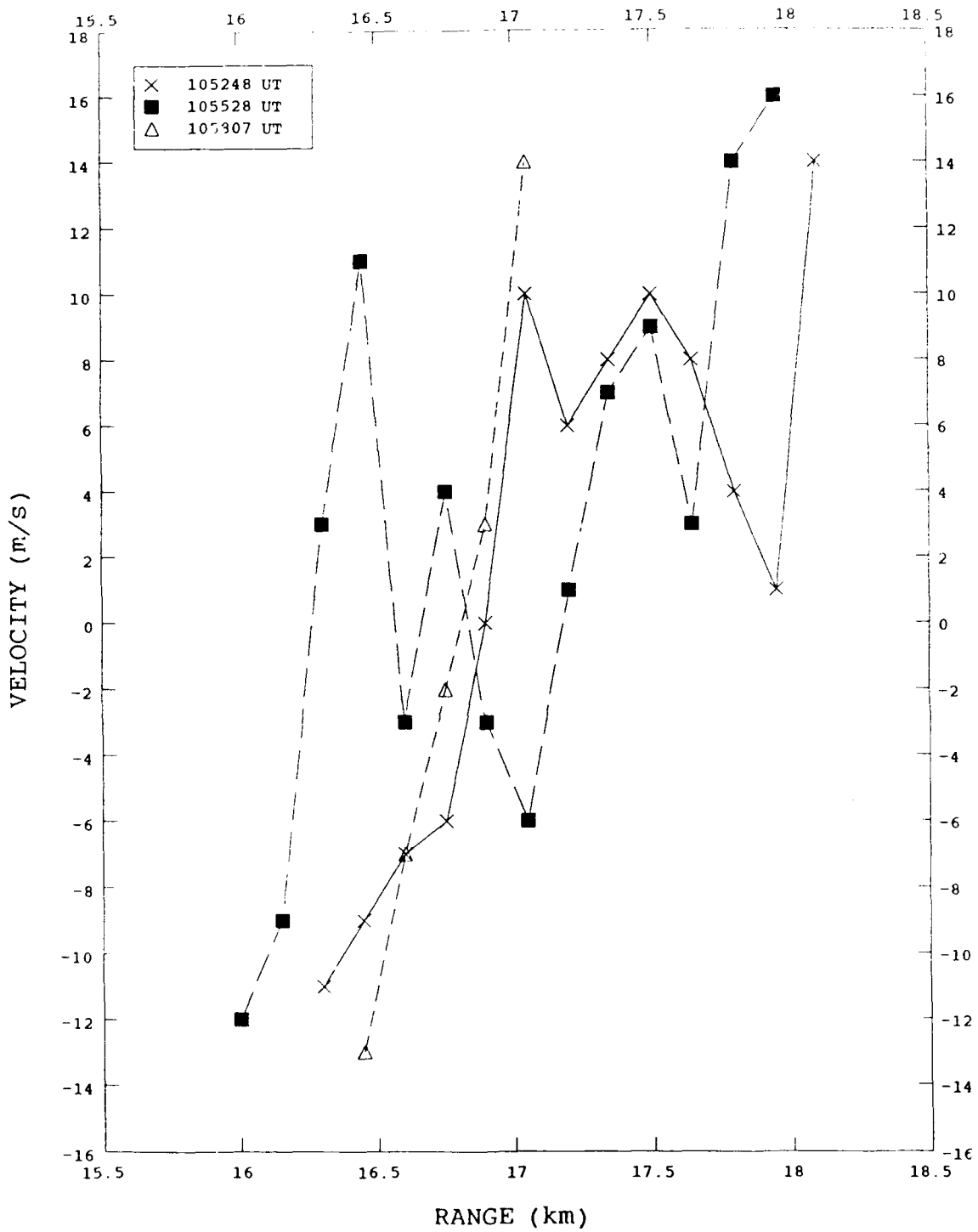
Figure 3. Plot of velocity vs. range of a birdburst on 12 September 1990 in Orlando, Florida.

105528 UT. At 105807 UT, the gradient (45 m/s per km) is too steep and the size (0.6 km) too small for a microburst. In addition, there was no reflectivity echo above the surface associated with the event.

Figure 4. shows three velocity images and one reflectivity image of a birdburst on 29 July 1986 in Huntsville, Alabama. For this and subsequent velocity images, the negative velocities represent flow towards the radar, while the positive velocities are flow away from the radar. The size of the velocity signature increases significantly with time, but the center of divergence remains the same. The reason the center of divergence did not change is that the event was caused by birds departing in the early morning hours from an overnight roosting site (Rinehart, 1986). In this case the site was a small island in the Tennessee River. This phenomenon occurred on a regular basis during the 1986 TDWR testing in Huntsville. Between 101650 and 104719 UT, the maximum velocity differential of this event changed very little. The highest reflectivities are near the edge of the echo with lower reflectivities in the center. The low−reflectivity notch signifies very few scatterers in the center of the departure waves.

In order to further characterize the birdburst phenomena, radar data was collected in the early morning hours of 9 December 1991 and 12 March 1992 in Orlando. Figure 5. shows the reflectivity and velocity characteristics of the 9 December 1991 case. At 113922 UT the birdburst which is located at 36 km and 190 degrees has a velocity differential of 16 m/s. The maximum surface reflectivity is 25 to 30 dBz. The signature is somewhat small at this time. A minute and one−half later the event size has more than doubled. The velocity differential is 20 m/s. There is a smaller, secondary wave of birds located just east of the main wave. Notice how the signature at 114047 UT is ragged with holes in the echo. The fact the echo does not completely fill all of the radar bins is a significant characteristic of a bird signature. This characteristic is also apparent in the event from 12 March 1992 (Figure 6.). The maximum velocity, maximum surface reflectivity and location are similar to the birdburst from 9 December. Both of the signatures were detected in the vicinity of a lake.

This data was presented to show there will not always be one distinguishing characteristic to differentiate birds from weather. Nevertheless, it is important for radar meteorologists to understand the cause for the echoes they are observing in order to design an appropriate algorithm to detect the phenomena.

A 1987 study by Larkin and Quine identified 11 potentially significant diagnostic variables for distinguishing bird echoes on radar. They are in the process of refining an automated algorithm for the Next Generation Weather Radar (NEXRAD) which can identify and classify biological echoes such as migratory birds. It should be stressed that the parameters identified by Larkin and Quine have not been fully tested on roosting birds. Among their most important findings were the following:

- Weather generates an echo region which is generally more widespread than birds. Biological targets do not conform to the model for water droplets, which would predict a slope of approximately $1/r^2$. The power
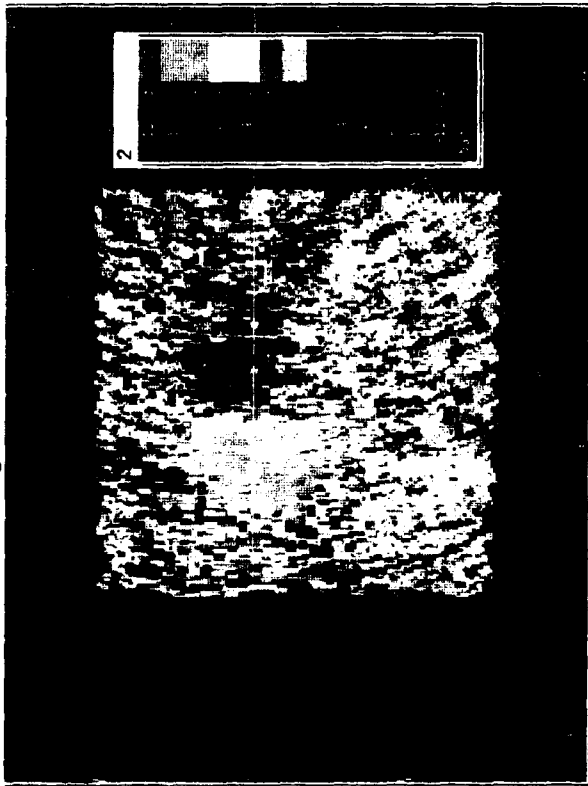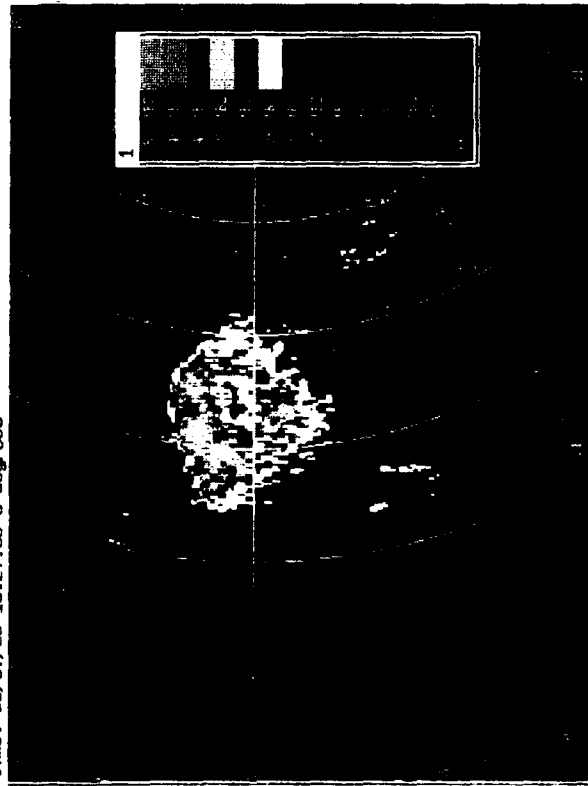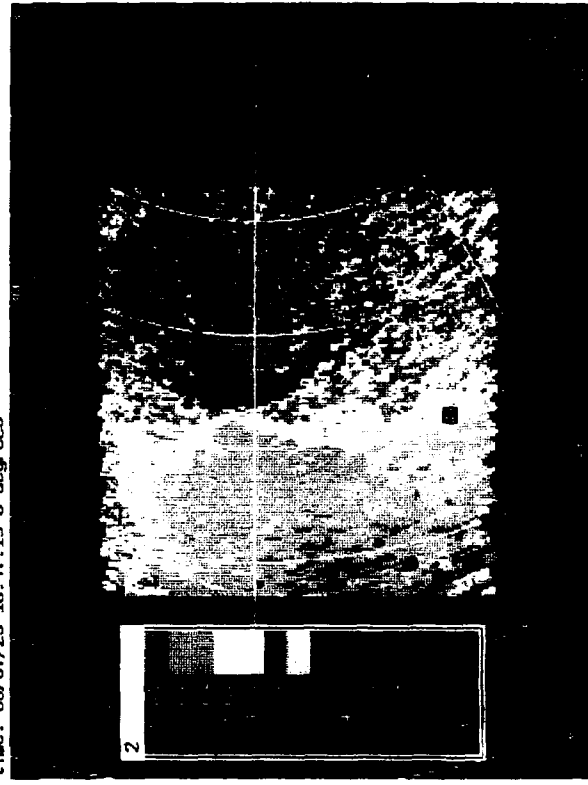
10
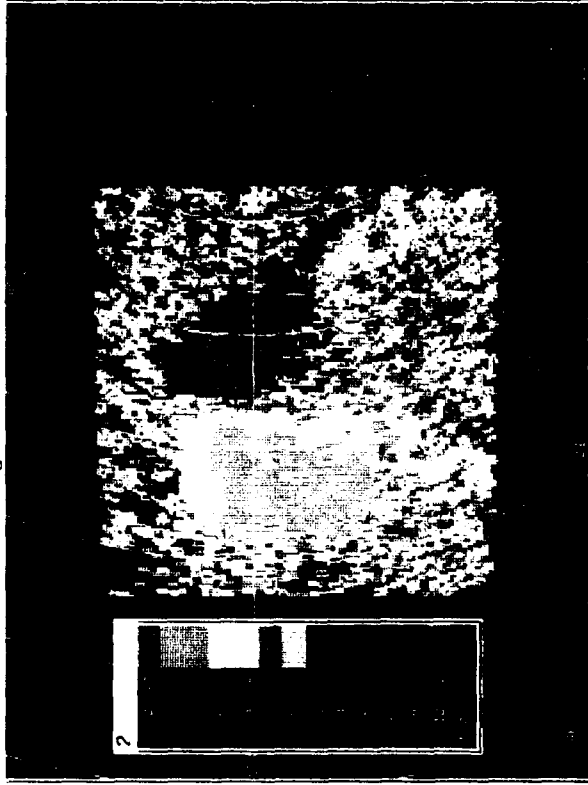
Figure 4. Reflectivity and velocity images of a birdburst on 20 July 1986 in Huntsville, Alabama.
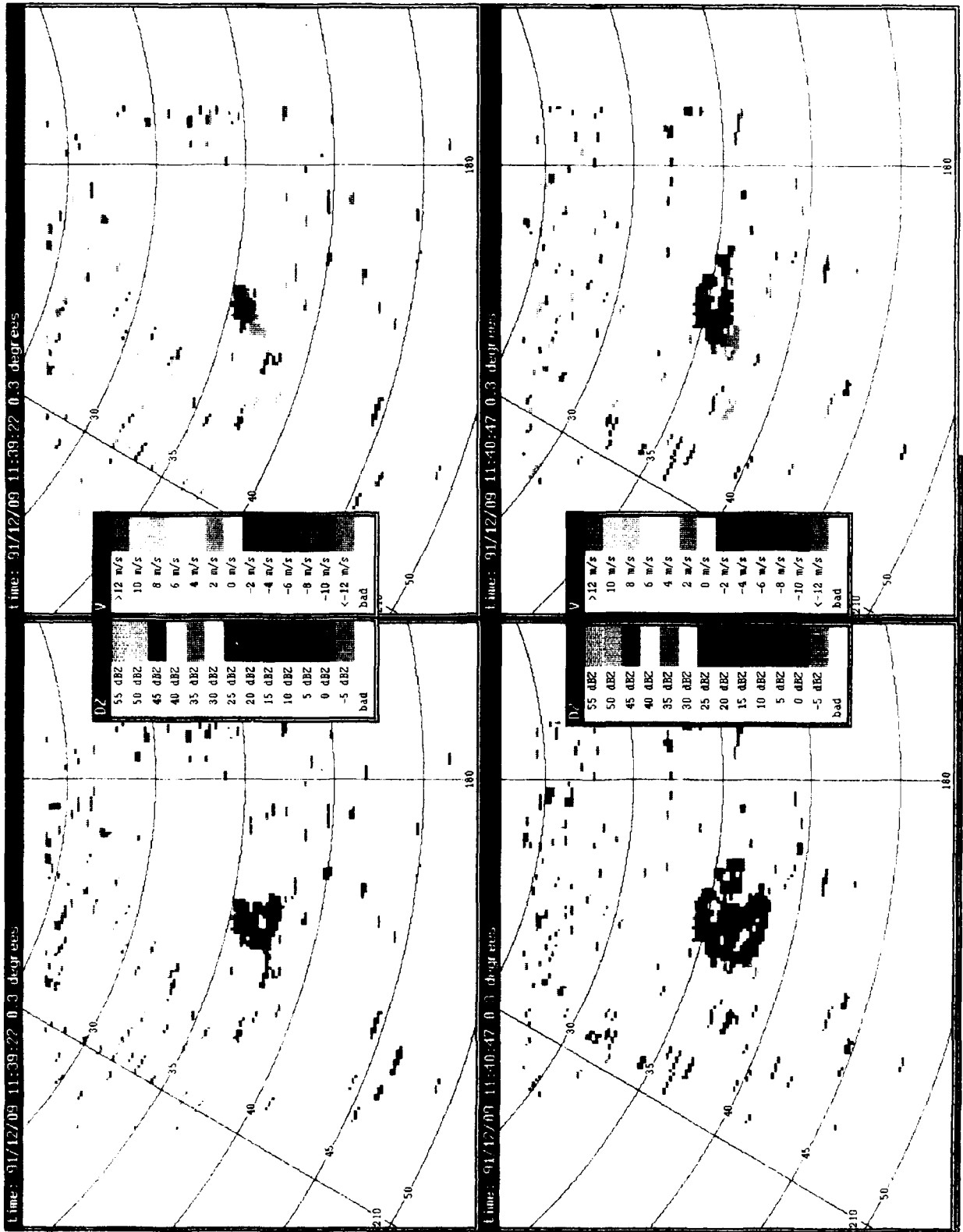
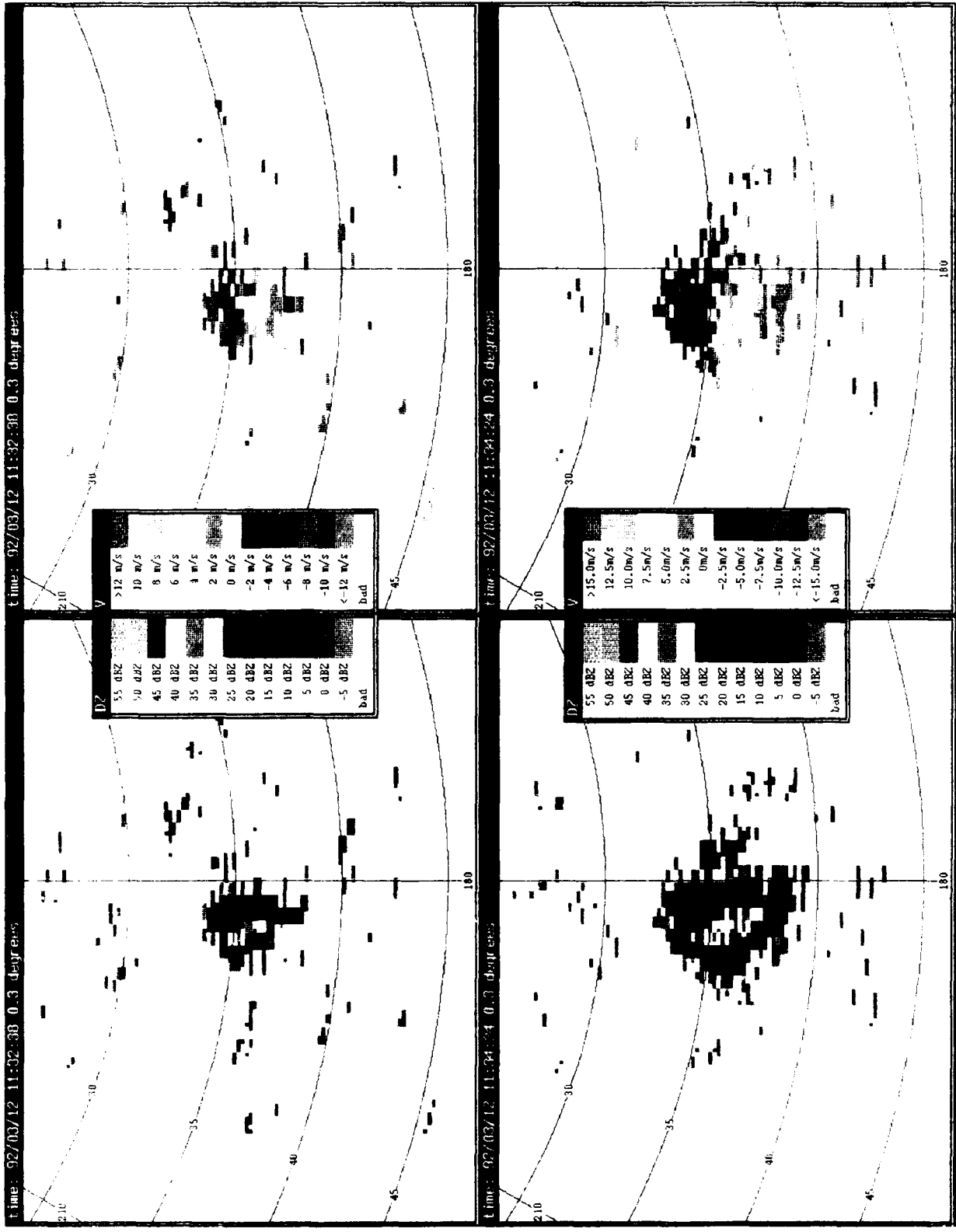*Figure 5. Reflectivity and velocity images of a birdburst on 9 December 1991 in Orlando, Florida.*

Figure 6. Reflectivity and velocity images of a birdburst on 12 March 1992 in Orlando, Florida.

15

returned to the radar from individual point targets such as birds decreases according to $1/r^4$.

- The degree of stipple in reflectivity, velocity and spectral width is greater in biological targets than in weather. According to Larkin and Quine, stipple is calculated by differentiating along each radial in a patch of echo and subtracting out the expected slope between the minimum and maximum value. The expected slope is defined as

$$\frac{2 \left(\text{maximum dBz} - \text{minimum dBz} \right)}{\text{number of range gates} - 1}$$

Stipple is defined as

$$\frac{\left(\text{accumulated differences in absolute reflectivity} - \text{the expected slope} \right)}{\text{number of range gates}}$$

They found, for instance, that the reflectivity stipple in migratory birds was generally > 4 dB, while weather was typically < 4 dB.

- The reflectivity and velocity images of bird echoes exhibit a "graininess" that is almost never present in weather. This is due to a small number of birds per range gate (including cases where birds are absent from some range gates). Therefore, the coverage of weather is nearly 100 percent, whereas the coverage of bird echoes is somewhat less, depending on the type and number of targets.

- Variance or spectral width may also be useful since bird echoes generally have lower spectral widths than weather. They found, for instance, that the average spectral width of migratory bird echoes, such as Canadian Geese, was < 1 m/s, while the spectrum width of weather echoes generally ranged between 3 and 5 m/s.

- The event location may be important since a bird echo may present a characteristic signature in the same location and possibly at the same time of the day. For instance, blackbirds in Illinois have been observed departing from the same location in nearly circular patterns around sunrise each morning (Larkin and Quine, 1989).

In this section, the diagnostic variables determined by Larkin and Quine will be further evaluated. The distribution of power returned to the radar from a bird target is highly dependent on the number of scatterers in the sampling volume. The $1/r^4$ rule only applies if there is

17

one bird per range sampling bin. If there are multiple birds, as typical with a large flock like the Huntsville case, the slope would be closer to either $1/r^3$ for a disk–shaped scatterer or $1/r^2$ for a 3D volume filling scatterer such as rain clouds. While this was not verified with the events examined here, it was assumed there were multiple birds within a range sampling bin based on the size and coverage of the echoes. Also, the lower spectral widths in migratory birds is due to a few birds in each range sampling bin which are flying in the same direction at a relatively constant speed. There may be distinct differences between the variance in the migratory birds studied by Larkin and Quine and the variance of roosting birds which may have caused the 2 June divergences. If the birds were scattering in all directions from a central location, there would probably be a higher variance just like in the center of a microburst.

3. CHARACTERISTICS OF 2 JUNE 1990 DIVERGENCE SIGNATURES

Table 2. shows statistics from all of the divergence signatures on 2 June in Orlando. It is hypothesized that each divergence signature on this day was caused by birds. The maximum delta V (differential velocity) of the events ranged from 11 to 36 m/s, while the maximum reflectivity varied from 0 to 44 dBz. Most of the apparent divergences were relatively short—lived, lasting from 5 to 21 min. While events # 2, 4, 9 and 10 exhibited an echo aloft, the maximum reflectivity was 14 dBz or less. In fact, the strongest apparent divergence on this day (# 2) had a maximum reflectivity of only 14 dBz. Almost all of low—reflectivity microbursts in Denver, Colorado, during 1987 and 1988 had a maximum reflectivity higher than this. The low reflectivity of most of these apparent divergences in a moist environment like Orlando was a good indication they were not caused by weather. An examination of the vertical reflectivity structure of each event revealed that four (6, 7, 8 and 11) were not accompanied by a reflectivity cell aloft. The lack of reflectivity aloft is the best method of distinguishing a weather from a non—weather echo. In fact, a storm cell validation test is used by the TDWR microburst algorithm to eliminate potential false alarms from non—weather divergences produced by birds or clutter. A storm cell in the TDWR is defined as a 3D echo region with a maximum reflectivity of at least 30 dBz. The cell must have an area of 4 km^2 and a depth of 0.5 km or more.[*] It was implemented after the Kansas City TDWR testing due to the high number of microburst algorithm false alarms (Evans, 1990).

There were no microburst alarms issued by the TDWR for the divergence signatures observed on 2 June based on the lack of a storm cell. If any of the events were microbursts, then the storm cell test would be detrimental to the algorithm's performance. However if they were birds, then the cell test achieved its objective. One characteristic of previous birdbursts which was not exhibited in the 2 June divergences was the time of occurrence. All of the events from this day were detected early in the afternoon. Just because the events did not occur near sunrise does not preclude the possibility that they were birds. In fact, the data from Kansas City suggests birdbursts can occur at other times of the day.

---

[*] The reflectivity, area and depth, as well as the use of the storm cell validation test, are site—adaptable parameters. The values shown here are viewed as nominal values for a wet microburst environment such as central Florida.

Table 2.
Characteristics of Divergent Signatures from
2 June 1990 in Orlando, Florida

Event #	Location (Range/ Azimuth)*	Start Time (UT)	Stop Time (UT)	Duration (min)	Delta V (m/s)	Max Refl (dBz)	Refl Aloft	Event Location
1	4.5/156	1830	1839	9	16	44	Y	Lake
2	22.7/140	1830	1849	>19	36	14	Y	Orange Grove
3	17.5/150	1837	1858	21	27	29	Y	Orange Grove
4	21.9/146	1846	1854	8	14	12	Y	Orange Grove
5	14.9/190	1851	1912	21	32	42	Y	Field
6	25.5/158	1830	1838	8	21	8	N	Lake
7	20.4/175	1832	1838	6	11	6	N	Swamp
8	28.2/159	1848	1853	5	15	0	N	Swamp
9	23.7/144	1848	1854	6	12	11	Y	Trees
10	23.8/141	1856	1904	8	13	7	Y	Orange Grove
11	23.7/194	1859	1904	5	11	7	N	Field

* Range in kilometers; azimuth in degrees.

20

4. 2 JUNE 1990 REFLECTIVITY, VELOCITY
AND SPECTRAL WIDTH DATA

In this section, two of the higher reflectivity divergences (events # 3 and 5) which were associated with an echo above the surface will be further analyzed. The co–location of the surface divergence and a low–reflectivity cell aloft made distinguishing between true microbursts and bird movements more difficult. This analysis will consist of a comparison of the velocity, reflectivity and spectral width profiles of the two divergences from 2 June with a low and high–reflectivity microburst profile. The emphasis will be to determine if there were any significant radar characteristics which can discriminate a bird echo, even if there was a weather echo in the same location.

4.1 Event # 5 — Velocity Profile

Figure 7. is a plot of the radial velocity at the surface versus range for the radial containing the strongest velocities in event # 5 at 185831 UT. The maximum velocity differential at this time was 26 m/s (−16/+10). It occurred over a distance of 2.8 km. The velocity profile shown in this figure is characteristic of a microburst e.g., increasing velocities with range over a short distance. The only anomaly is the large velocity jump of 6 m/s located between 14.15 and 14.3 km (A). It coincides with velocities near 0 m/s and was probably caused by the clutter suppression filters which notched out the weaker velocities. The fact that there is a greater slope in the center of the velocity signature has also been observed with microbursts detected by the TDWR testbed radar.*

Figure 8. shows the radial velocity and reflectivity signature of this event. At 185008 UT, a weak divergent signature is located at 15 km and 190°. The maximum velocity differential is less than 10 m/s. In the next minute, the velocity differential has increased to 14 m/s. By 185228 UT, there is the classical microburst signature of a 20 m/s velocity differential (−10/+10) over a distance of 1.4 km. The maximum surface reflectivity at this time was 30 to 35 dBz.

Figure 9. is a plot of the divergence (delta V) and shear (DV/DR) for each minute event # 5 was above the minimum velocity threshold (10 m/s) for a microburst. The divergence peaked at 32 m/s and maintained a velocity differential of 20 m/s for a period of 12 min. The shear, on the other hand, peaks twice at +2 and +8 min. The peaks in shear correspond to a time of the minimum delta R (not shown) and maximum delta V. The maximum shear produced by this divergence would represent a considerable aviation hazard if it 1) was a microburst and 2) was encountered at low levels along the flight path.

4.2 Event # 5 — Spectral Width Profile

In a study of migratory birds by Larkin and Quine (1989), the spectral width or variance of the velocities was used to differentiate migratory birds from weather. As previously reported,
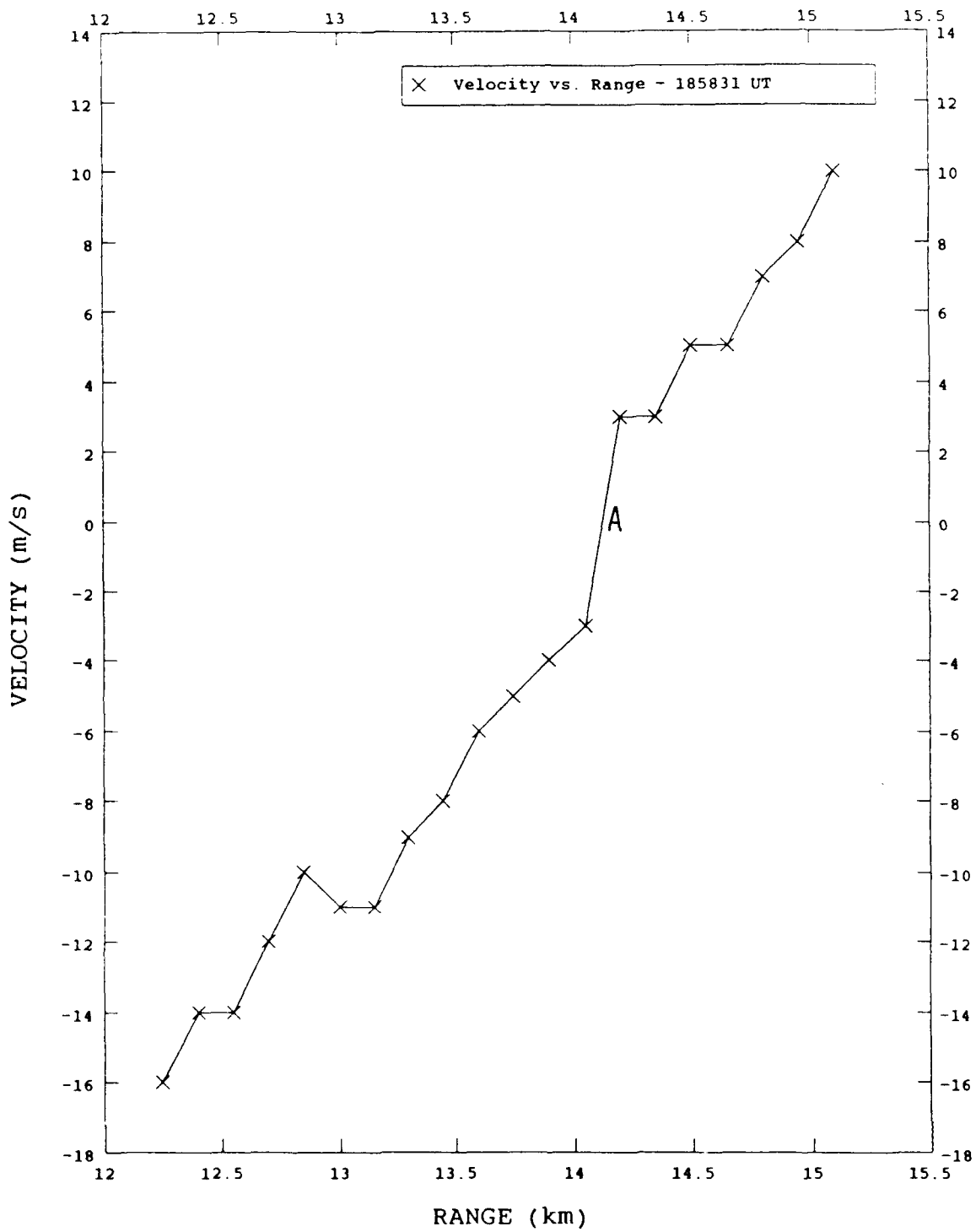
---

* For example, see figure 3 in Merritt, 1989.

Figure 7. Plot of velocity vs. range of event # 5 at 185831 UT on 2 June 1990 in Orlando, Florida.
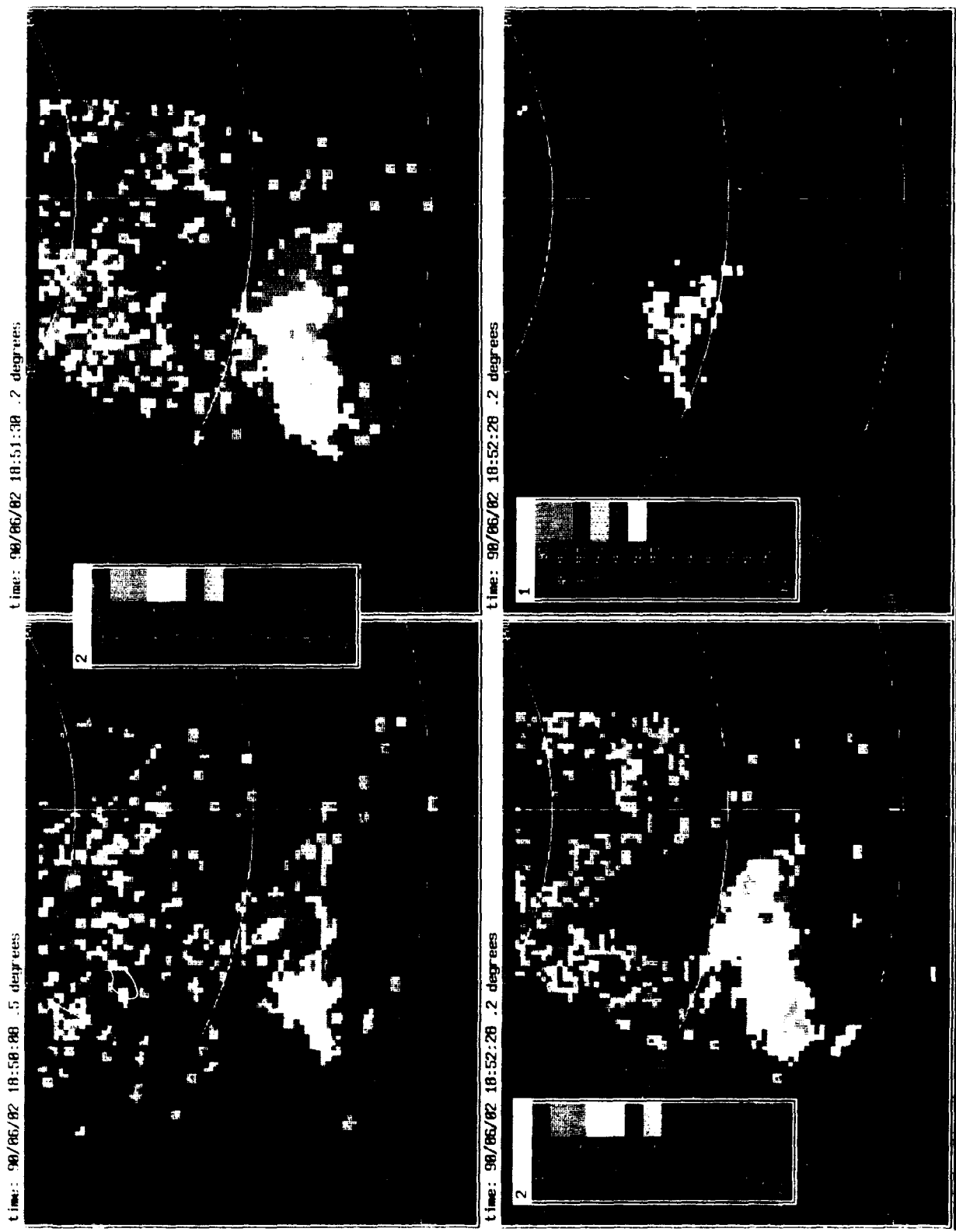
Figure 8. Reflectivity and velocity images of event # 5 on 2 June 1990 in Orlando, Florida. The velocity images show the time evolution of the low-level velocity features over a 2.5-minute period. The reflectivity image shows the low-level reflectivity at the time of the maximum delta V.
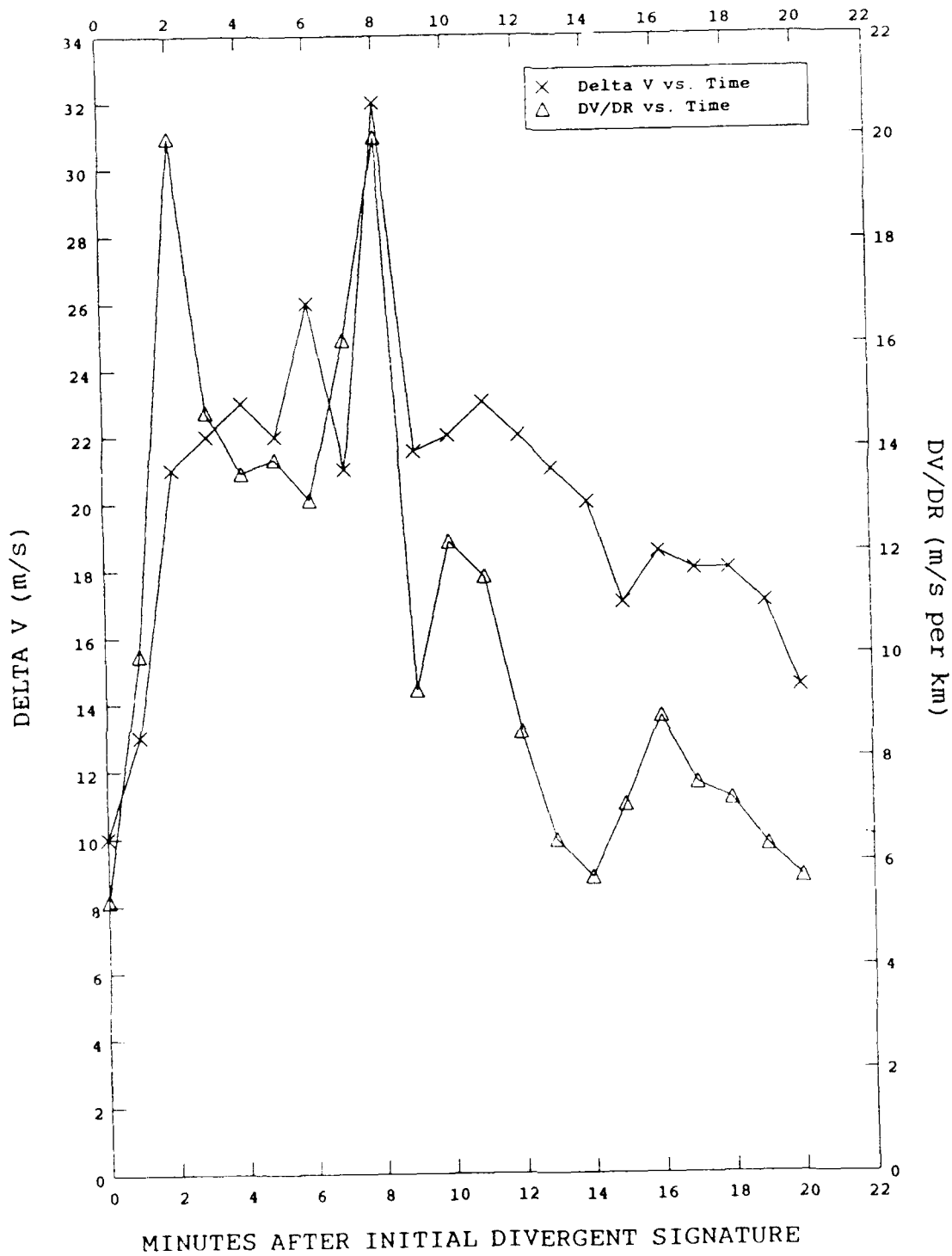
Figure 9. Plot of delta V and DV/DR vs. time of event # 5 on 2 June 1990 in Orlando, Florida.

25

they concluded that the average spectral width of Canadian Geese was typically less than weather. For this analysis, the average spectral width between a microburst and event # 5 was compared. In contrast to the results of Larkin and Quine, the average spectral width was slightly less in the weather case, e.g., 1.7 versus 2.1 m/s. At least for this one event, there was no way to determine its cause based on the average spectral width. Therefore, it was not included as an analysis technique for the other event. It may still prove to be a useful diagnostic tool for discriminating some types of weather, e.g., stratiform precipitation from migratory birds.

4.3 Event # 5 − Reflectivity Profile

An examination of the horizontal surface reflectivity profiles of event # 5 showed a consistent asymmetrical pattern, with the maximum reflectivity located near one edge of the echo. This type of asymmetrical pattern in the reflectivity field could serve to distinguish birds from microbursts. This theory was tested by comparing the reflectivity profile of several microbursts with the two events from 2 June 1990. The profile of a low−reflectivity Denver and high−reflectivity Orlando outflow are shown in Figure 10. While the reflectivity curve in the Orlando event is much steeper, both are characterized by the peak reflectivity near the middle and lower reflectivities on the ends. It should be pointed out that this type of pattern will not always occur with weather. For instance, strong environmental winds or strong updrafts/downdrafts would tend to skew the reflectivity distribution. One example of an asymmetrical horizontal reflectivity distribution with weather would be a high−reflectivity bow echo.

Four surface reflectivity profiles of event # 5 are shown in Figure 11. At 185130 UT, when the divergence is still weak, the maximum reflectivity of 35 dBz is located near the center. As time progresses, the maximum reflectivity is detected closer to the edge of the echo. By 185831 UT, it is located in the second range gate of the signature. This type of asymmetrical reflectivity profile is not indicative of the two weather examples which were previously discussed, especially if the maximum reflectivity is located in the first few range gates.

The vertical distribution of the location of the maximum reflectivity for this event is shown in Figure 12. Once again, it is dominated by the maximum reflectivity near the beginning of the signature, especially at a height of 2.7 km AGL and below. Above this altitude the profiles are more symmetrical. At least for this event, the pattern of reflectivity asymmetry was similar from the surface to 2.7 km AGL.

Figure 13. is a contour plot of surface reflectivity for event # 5 at 185331 UT. There is a sharp gradient along the northwestern edge of the echo (A). The maximum surface reflectivity is between 30 and 35 dBz. This clustering of the highest reflectivity near the edge of the echo was also observed in the 29 July 1986 birdburst in Huntsville (refer to Figure 4.). While the maximum surface reflectivity of this divergence was greater than most of the other events on this day, it was still within the range for birdbursts reported in Table 1. In fact, the maximum surface reflectivity of this event was similar to the other birdbursts from Orlando.

Figure 14. is a plot of surface reflectivity and velocity for event # 5 at 190252 UT. The velocity profile displays the typical microburst pattern of increasing velocities with range, while
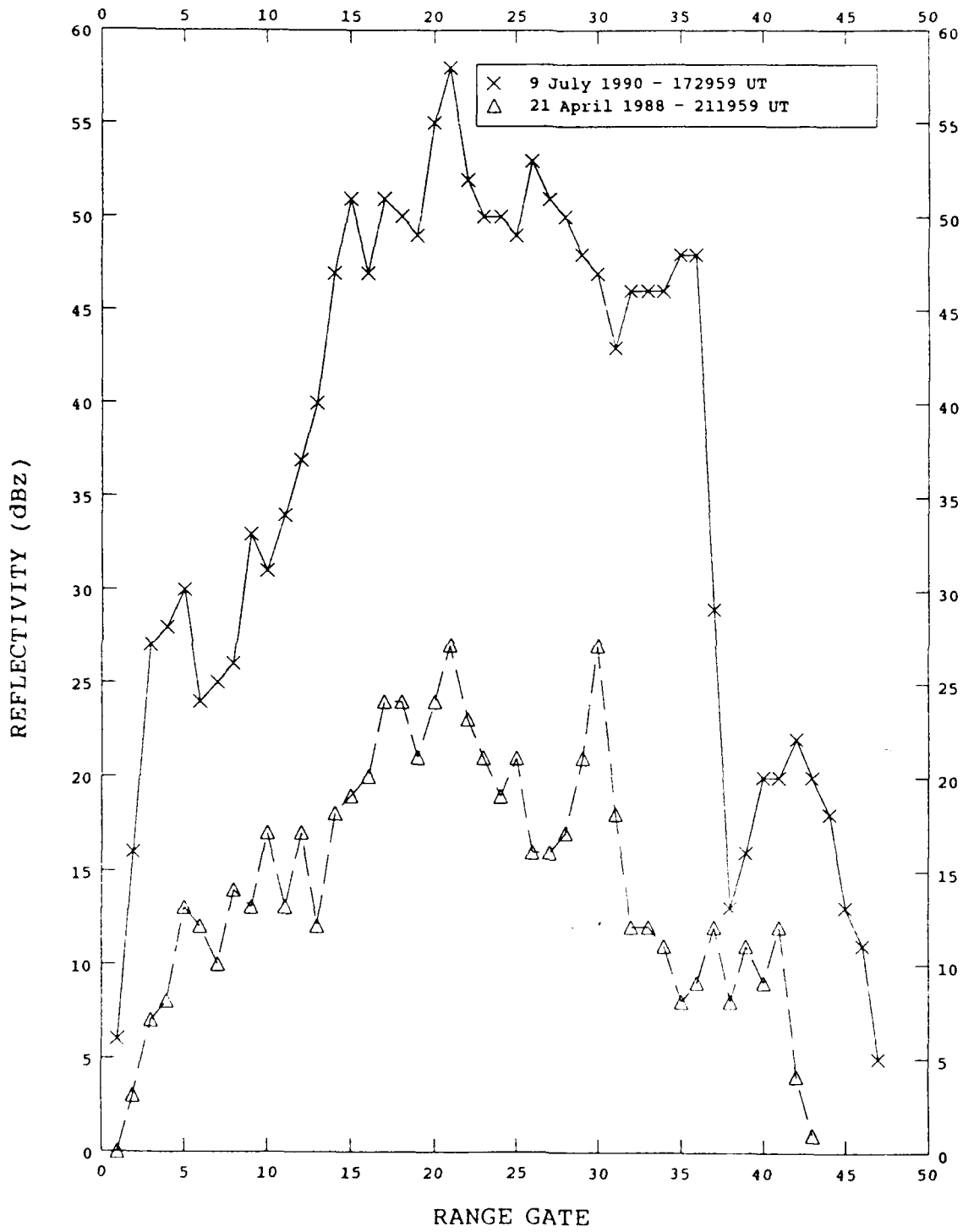
Figure 10. Plot of surface reflectivity vs. radar range gate of a microburst on 9 July 1990 in Orlando, Florida and 21 April 1988 in Denver, Colorado.
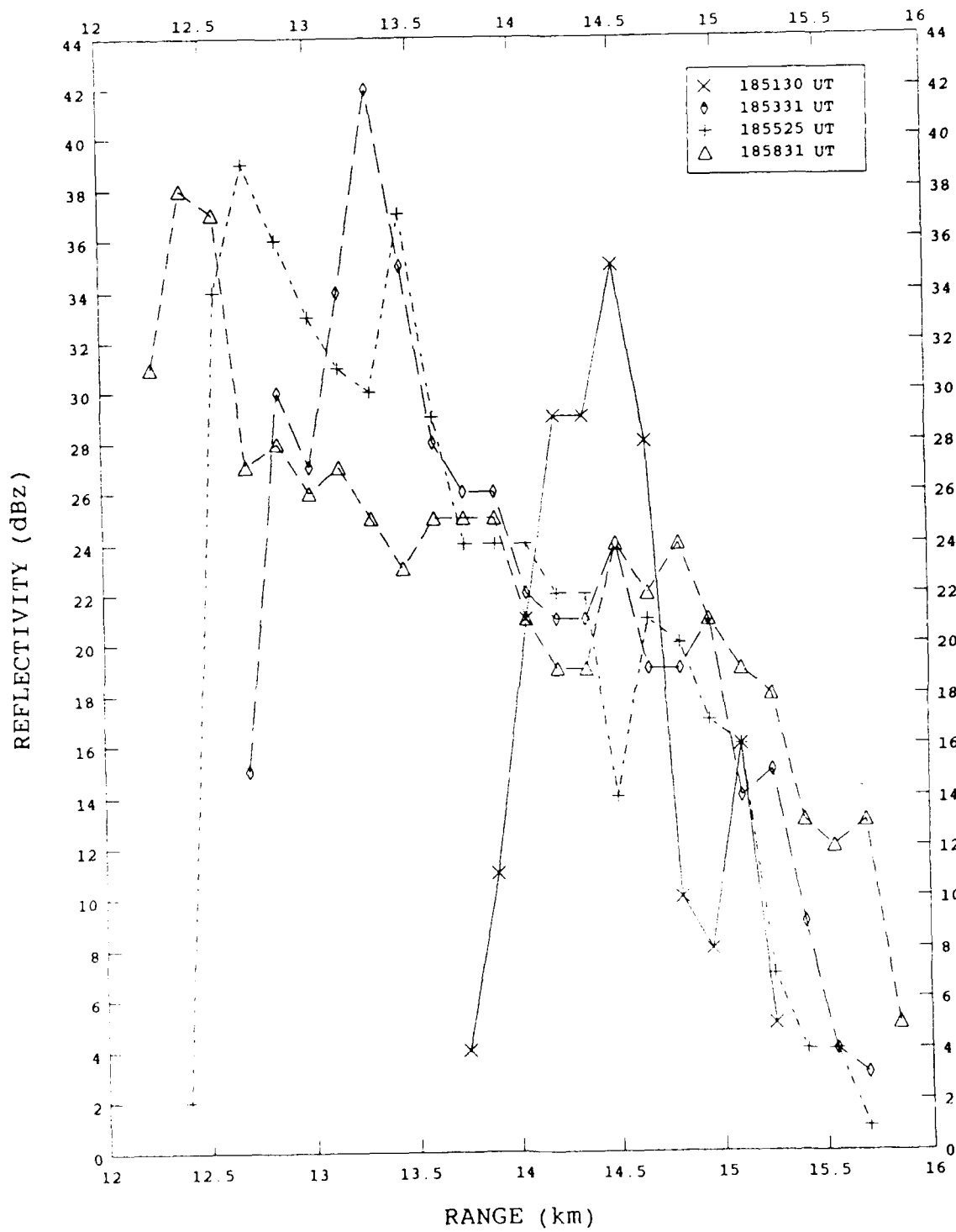
27

Figure 11. Plot of surface reflectivity vs. range of event # 5 on 2 June 1990 in Orlando, Florida.
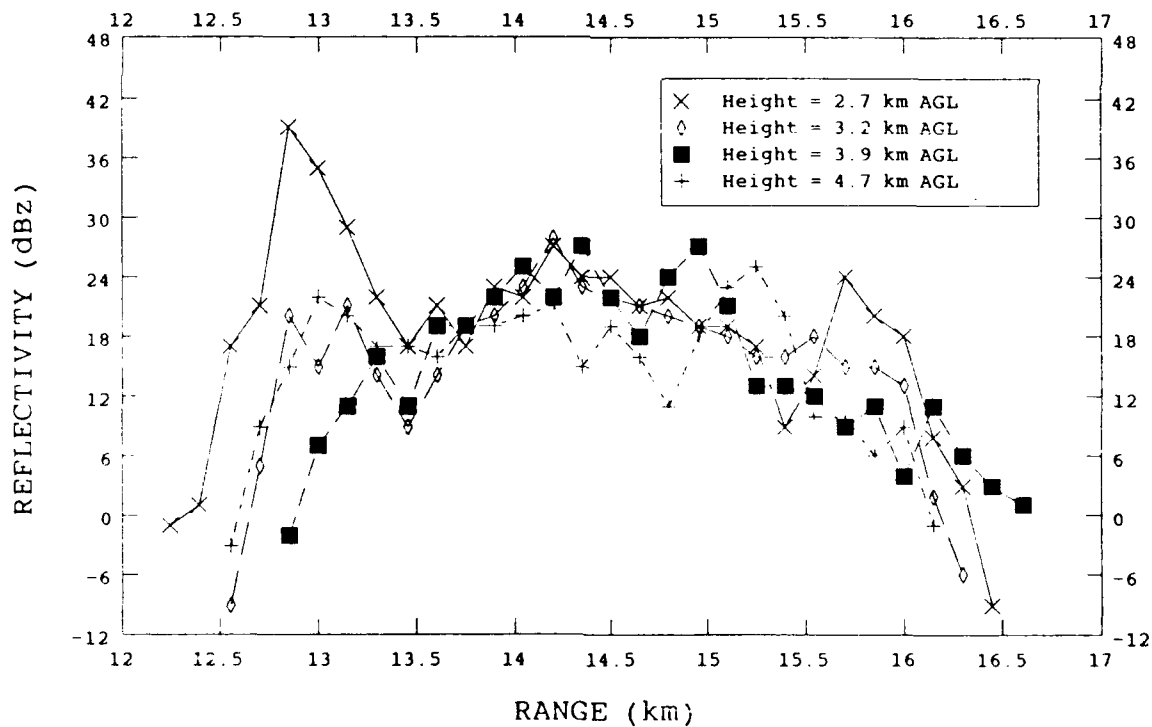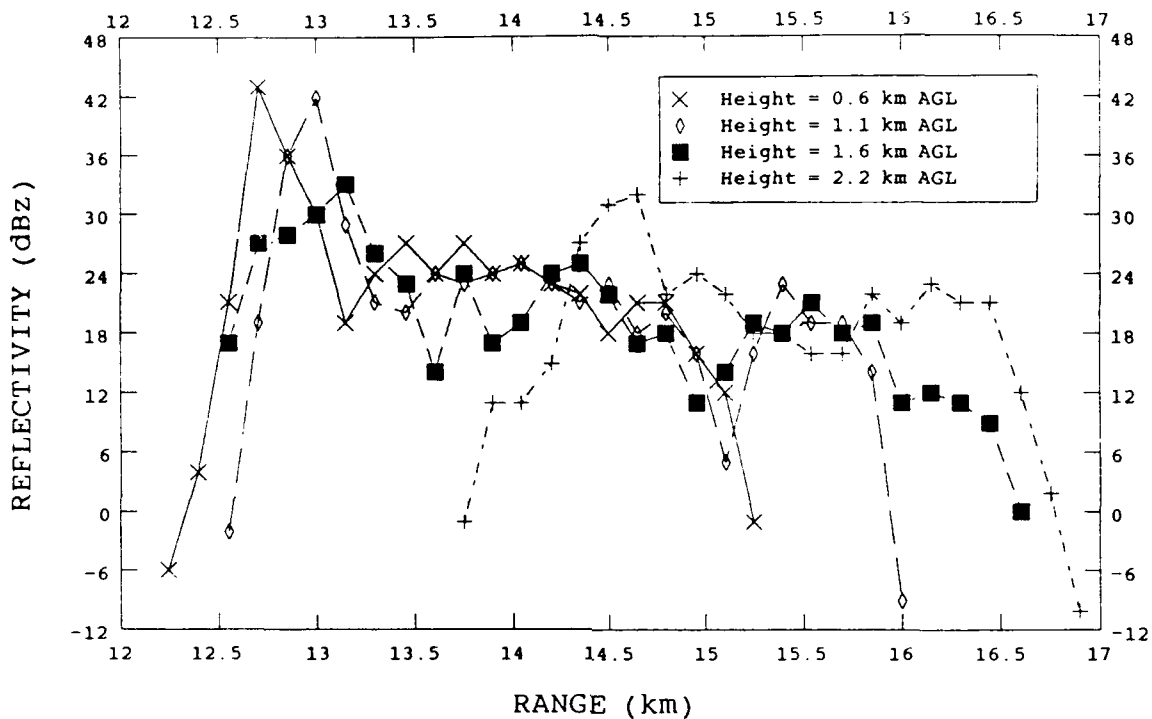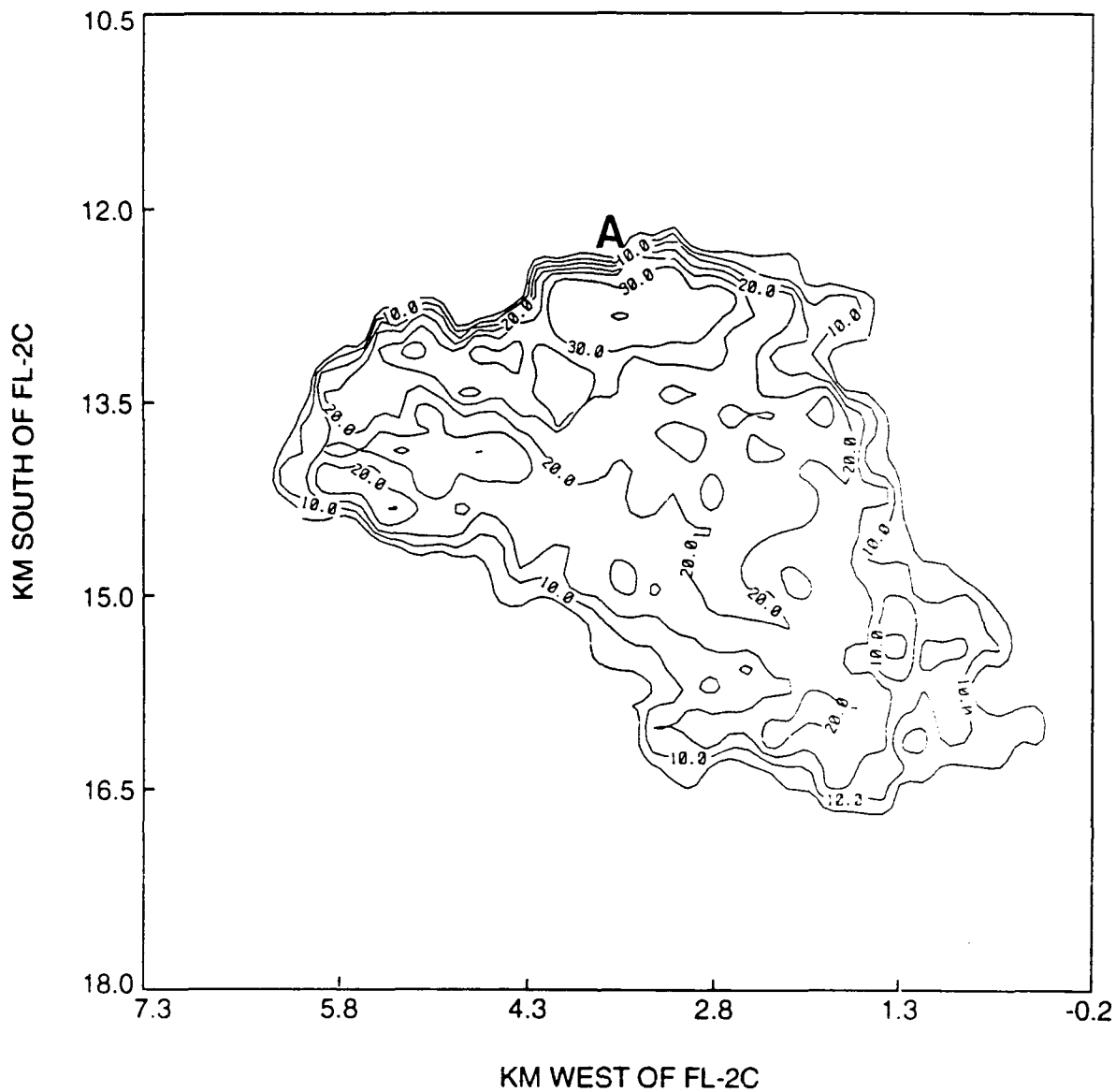
Figure 12. Plot of reflectivity aloft vs. range of event # 5 on 2 June 1990 in Orlando, Florida.

29

Figure 13. Contour plot of surface reflectivity of event # 5 at 185331 UT on 2 June 1990 in Orlando, Florida.

the reflectivity profile is strongly asymmetrical, with a sharp peak in the maximum approaching velocities and a secondary peak in the maximum receding velocities. The reflectivity decreases to 0 between the peaks. This type of reflectivity distribution is similar to the Huntsville Bird-burst which displayed a low−reflectivity notch between two reflectivity peaks. The co−location of the maximum reflectivity and velocity is not indicative of a microburst. It can easily be attributed to a large number of birds flying in opposite radial directions, which would be characterized by similar velocities and/or reflectivities in the same location. In this case, the maximum reflectivity of the echo approaching the radar exceeds the echo which is moving away.

30
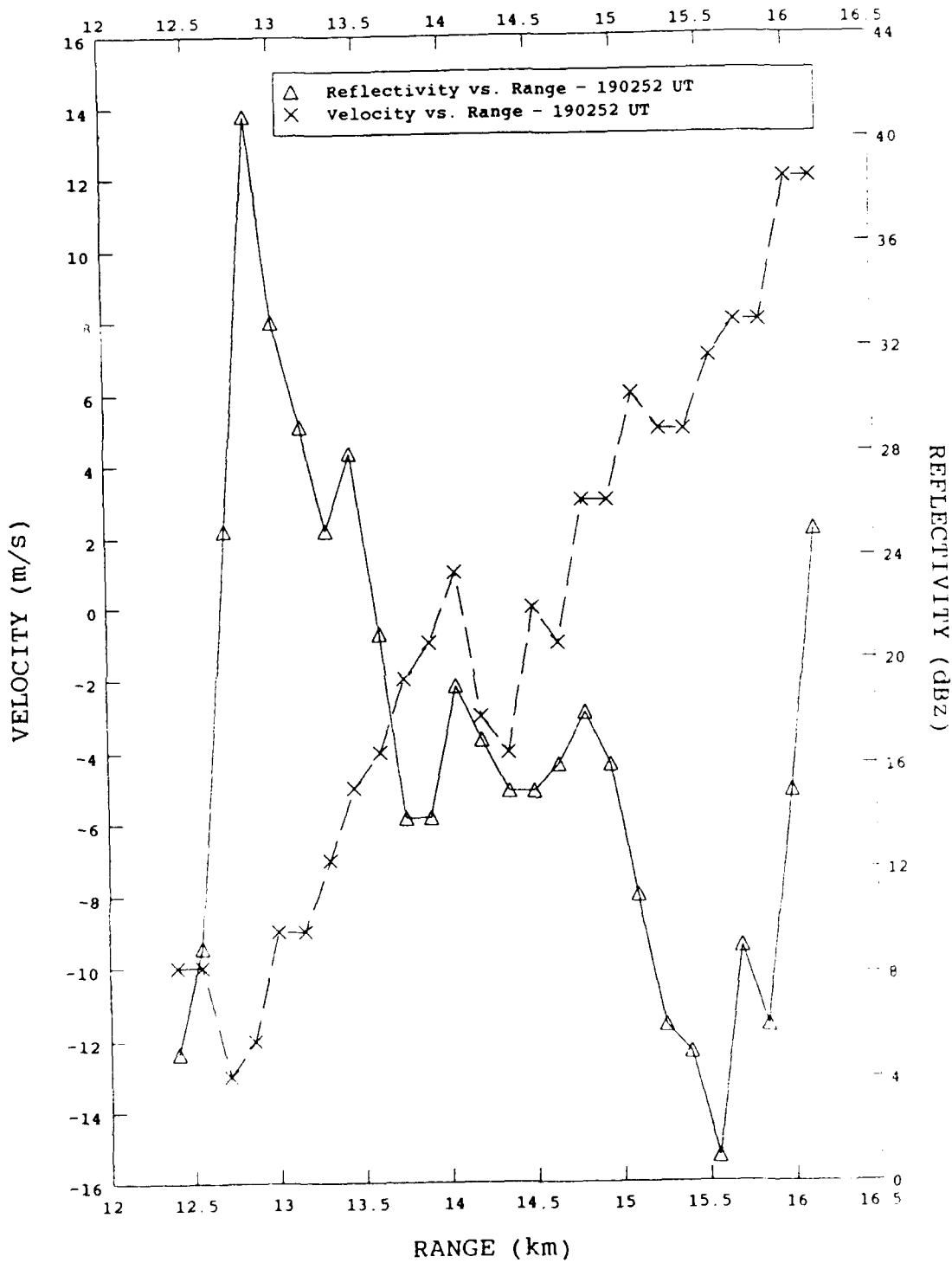
Figure 14. Plot of reflectivity and velocity vs. range of event # 5 at 190252 UT on 2 June 1990 in Orlando, Florida.

31

The fact that there is higher reflectivity on one side is consistent with the Huntsville Birdburst and the 9 December 1991 Orlando case.

4.4 Event # 3 – Velocity Profile

Figure 15. is a BSCAN** of the radial velocity for event # 3 at 184130 UT. The divergent signature is denoted by the rectangular box. The strongest velocity differential at this time is 27 m/s over a distance of 1.8 km (along the 155.5° radial). While this event is somewhat smaller than # 5, the velocity profile is still indicative of a microburst. Notice the larger velocity changes near the center of the outflow, especially at 155.5° and 156.5°. The steep gradient across the zero velocity region is similar to event # 5. Figure 16. shows three Doppler velocity images and one reflectivity image of this event. Over a three–minute period the maximum velocity differential increases from 15 to 27 m/s. At the time of maximum divergence, the maximum surface reflectivity was only 20 dBz.

4.5 Event # 3 – Reflectivity Profile

Figure 17. shows the horizontal surface reflectivity profile for event # 3 at three times. The curves show a steep rise to the peak reflectivity, which ranges from 27 to 29 dBz. After the peak, the reflectivity drops off gradually to a minimum of approximately 0 dBz. All three curves show the same asymmetrical pattern as event # 5, with the maximum reflectivity located near the edge of the echo. In the section which follows, the implication of this type of profile will be further analyzed.

4.6 Reflectivity Profile Synopsis of Events # 3 and 5

Figure 18. shows the location of the maximum reflectivity (percent length of segment) for all of the echoes at the surface and aloft associated with events # 3 and 5. A composite profile of 23 Orlando microbursts is shown to represent weather. The maximum surface reflectivity in the 2 June divergences was typically located within the first quarter of the segment. For example, approximately 70 perce⌐ of the segments in event # 5 contained the maximum reflectivity within the first quarter. The s face curve for this event is slightly more asymmetrical than # 3. By comparison, the maximum surface reflectivity curve in the Orlando microbursts was more symmetrical. While the maximum reflectivity of the average Orlando microburst was in the middle third of the distribution, there were some cases where the maximum surface reflectivity was located near the edge, but not to the degree exhibited with events # 3 and 5.

The distribution of the maximum reflectivity for the echoes above the surface associated with events # 3 and 5 is also shown in this figure. The curve for the echoes above the surface in event # 5 was similar to the surface curve, just not as pronounced. There was little difference in the location of the maximum reflectivity between the surface and aloft for this divergence.

** The BSCAN is a table of the radial velocity (m/s) versus range (on the horizontal axis) and azimuth (on the vertical axis).

PPI Tilt time 06/02/90 18:41:30 to 18:41:36 103 radials Scan 3 Tilt 10 Product V
Spacing = 150m Nyq. vel. = 22.35m/s Unamb. range = 89.7km

v

RANGE IN KM

Figure 15. BSCAN of velocity vs. range of event # 3 at 184130 UT on 2 June 1990 In Orlando, Florida.

PPI Tilt time 06/02/90 18:41:30 to 18:41:36 103 radials Scan 3 Tilt 10 Product V
Spacing = 150m Nyq. vel. = 22.35m/s Unamb. range = 89.7km

v

| time | elev | azm | 17.80 | 18.40 | 19.15 | 19.90 | 20.65 | 21.40 ray |

RANGE IN KM

Figure 15. (Continued).
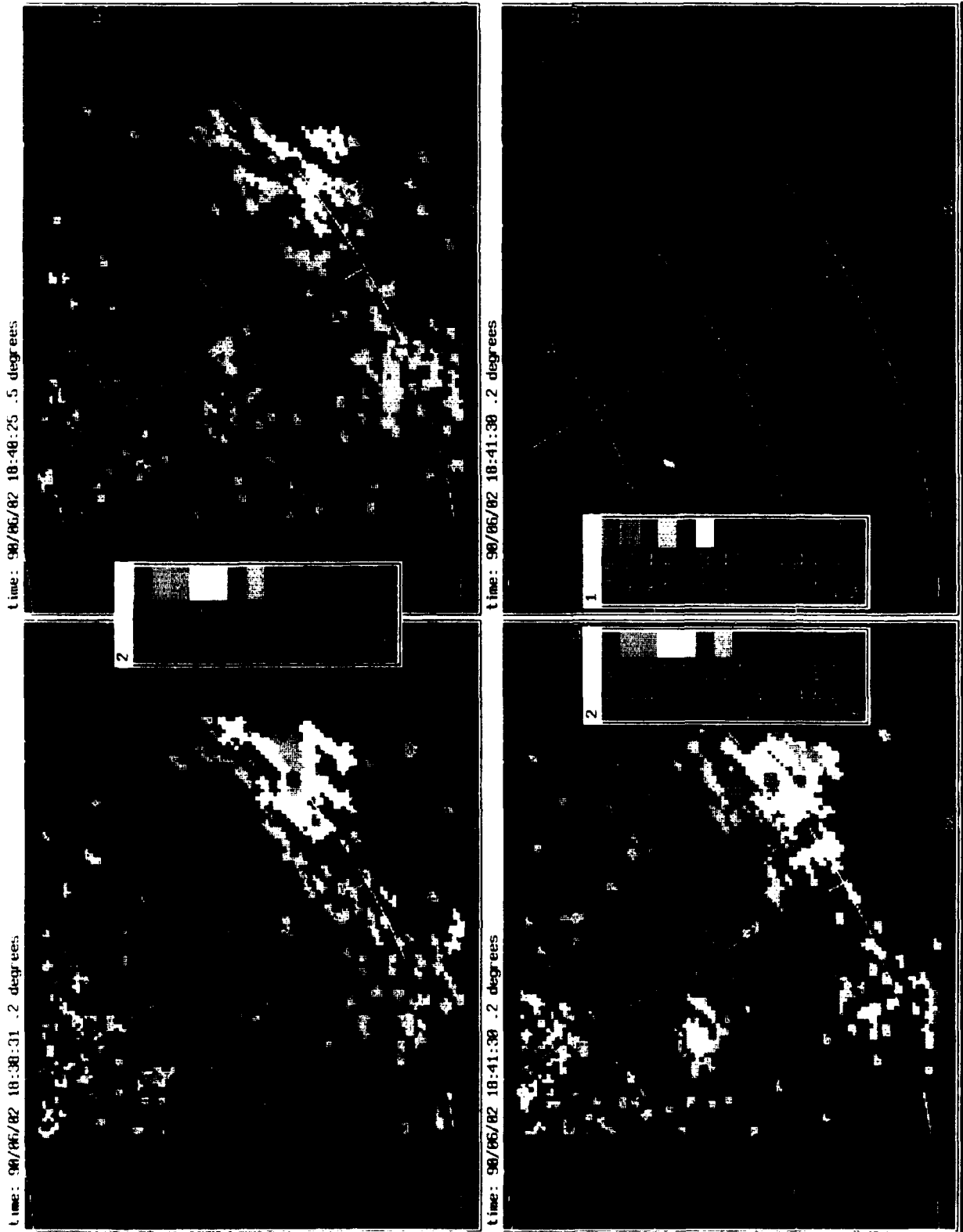
Figure 16. Reflectivity and velocity images of event # 3 on 2 June 1990 in Orlando, Florida.
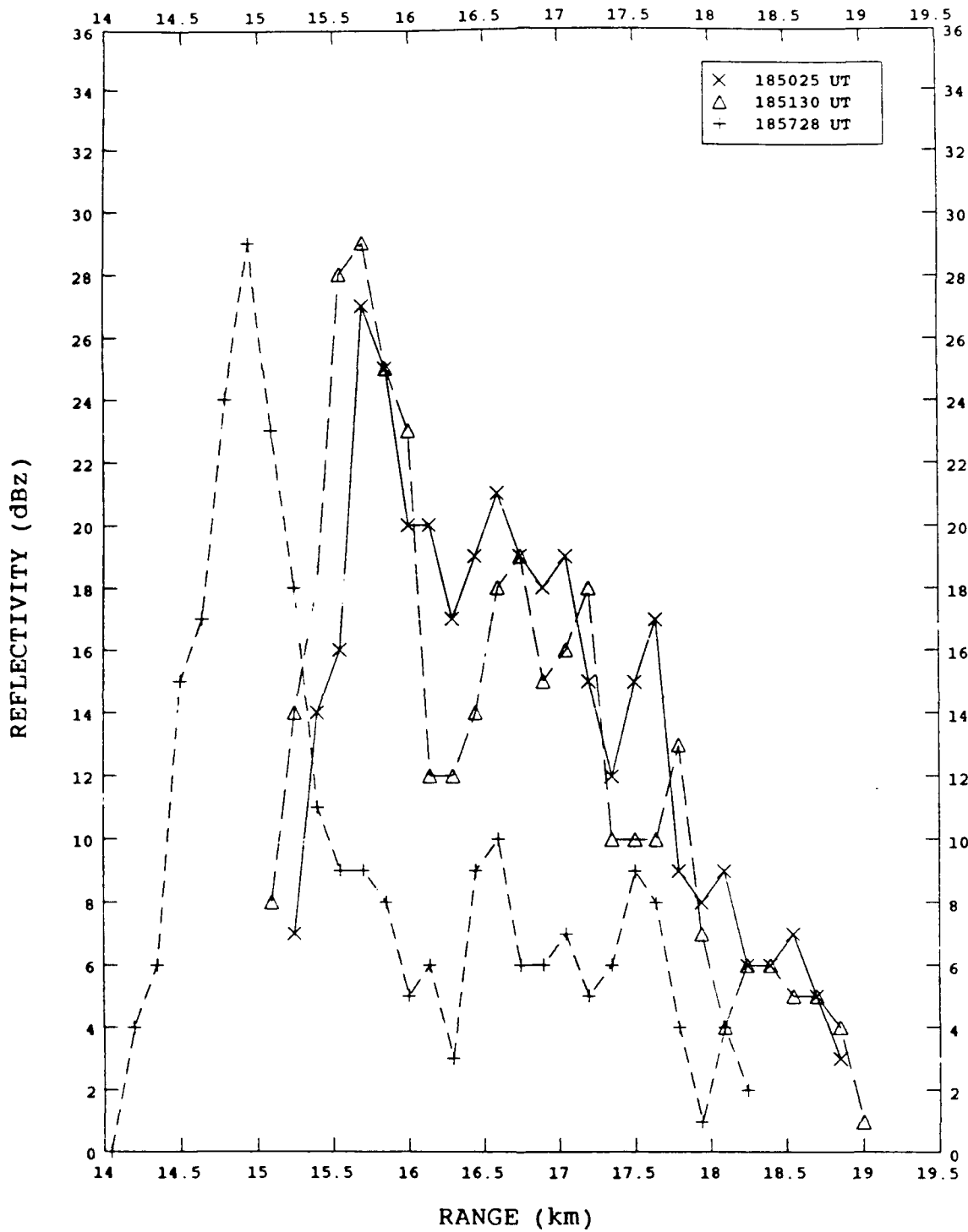
Figure 17. Plot of reflectivity vs. range of event # 3 on 2 June 1990 in Orlando, Florida.

37
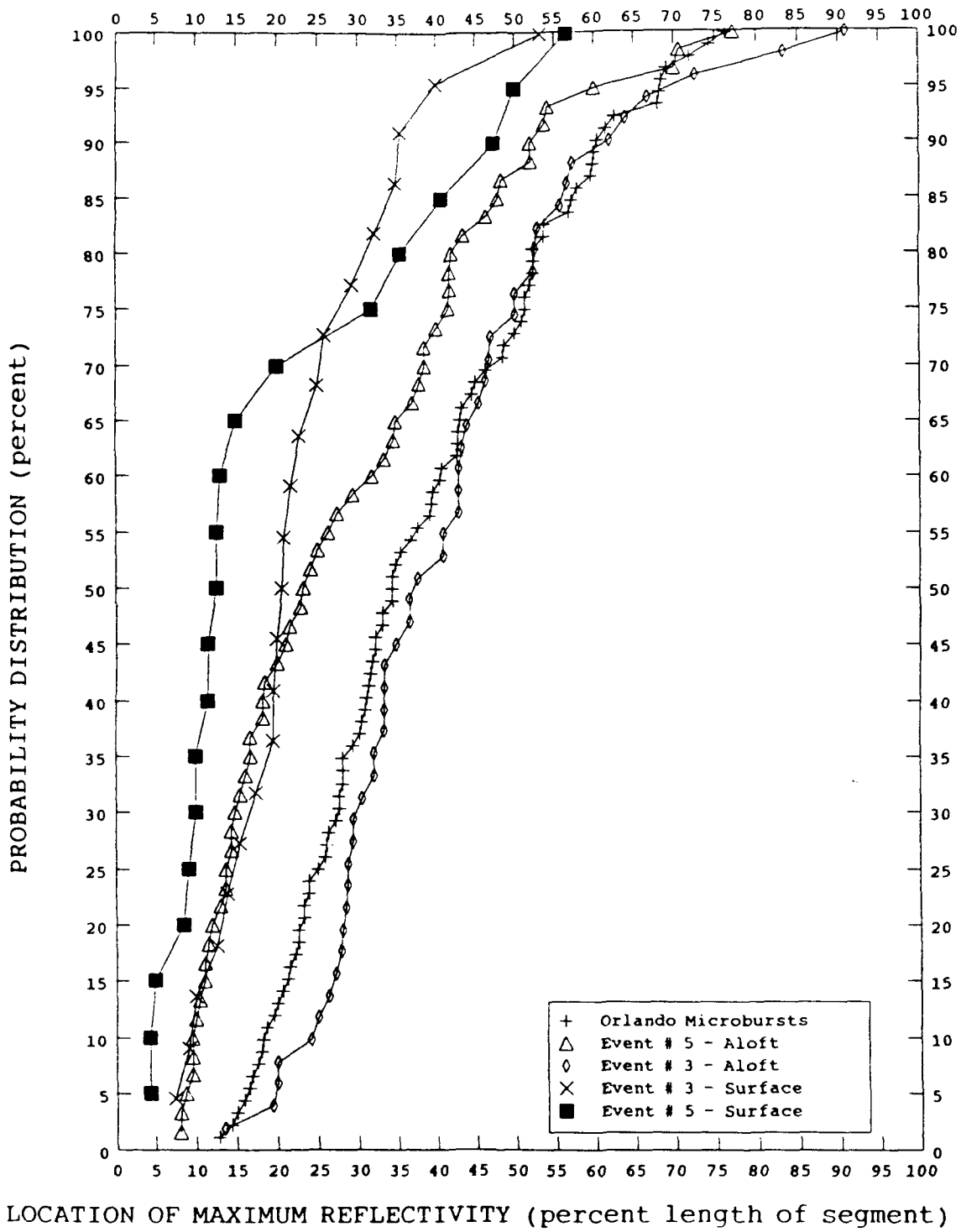
Figure 18. Plot of the probability distribution of the location of maximum reflectivity.

However, there was a significant difference noted between the surface and aloft curves for event # 3. The distribution of the maximum reflectivity aloft for this event was similar to the curve for the Orlando microbursts, as expected. This analysis suggests the location of the maximum reflectivity in a microburst may be encountered near the edge, but there were no examples of the maximum reflectivity within the first few range gates. An echo which exhibits the maximum reflectivity within the first few range gates of the signature, in combination with other information, could be used to distinguish birds from weather.

The physical mechanism which leads to a strong maximum reflectivity in dBZ at the near edge of the velocity signature is unclear. The reflectivity measurements reported here have been characterized by the dBZ value which uses an R^2 range normalization. As noted earlier, if the bird flock filled the beam resolution volume, there would be no range dependence of dBZ. If the bird flock filled the beam horizontally* but flew only in a narrow band of altitude, the dBZ reflectivity would drop off as 1/R. However, in figure 11, the dBZ reflectivity drops off much more rapidly (e.g., 15−20 dB, with a change in range of 10 percent to 20 percent) as one moves toward the center of the divergence. If the bird flock looked like a doughnut, we would expect high reflectivities (in dBZ) on the trailing edge as well as on the leading edge.

Two possible theories can be postulated to explain the higher reflectivities on the leading edge of the echo. First, the winds were east−southeasterly prior to these events. Therefore, the majority of birds flew in a northerly direction, which would be *with* the wind, especially for event # 3 which was located to the southeast. The second theory is that the majority of birds flew to the north to avoid the approaching rainshower. Both velocity signatures also showed the stronger velocities on the leading edge of the echo. Since similar species of birds would fly at approximately the same speed, the stronger velocities to the north would support the theory that more birds were flying *with* the winds. Thus, the higher reflectivity signature on the leading edge of the echo was caused by birds, while the lower reflectivities were probably weather.

---

* A good assumption, given that the signatures all encompassed a number of azimuths.

5. REFLECTIVITY STIPPLE

In this section, the method used to calculate reflectivity stipple, developed by Larkin and Quine, will be tested to determine if it can be used to distinguish roosting birds from weather. This analysis was based on the TDWR testbed range gate resolution which was 120 meters in 1988–1989 and 150 meters in 1990–1992. It should be noted that Larkin and Quine used a range gate spacing of 1 km for their calculations to be consistent with NEXRAD.

Figure 19. is a plot of the distribution of the average reflectivity stipple for weather, birds and events # 3 and 5 from 2 June 1990 in Orlando. The average stipple in the weather case was 3 dB, which is similar to the results of Larkin and Quine. By comparison, the average stipple for events # 3 and 5 from 2 June was 2.7 and 4.1, respectively. According to the results of Larkin and Quine, a stipple < 4 dB would be more representative of weather than migratory birds. One might conclude from these results that the events from 2 June, especially # 3, must have been caused by weather. However, there is additional data in the figure which might suggest otherwise. The average stipple for the two bird events from Huntsville and Kansas City was also < 4 dB and only slightly greater than the weather example. Therefore, it appears that the use of stipple to differentiate roosting birds from weather was not as significant as the results obtained with migratory birds.

Also shown in Figure 19. is the distribution of the average stipple for the echoes above the surface associated with event # 5. This data was analyzed to determine if the average stipple at the surface was significantly different from the average stipple above the surface for this event. The distribution was almost identical between the surface and aloft. This was consistent with the earlier results presented in Figure 12. which showed the asymmetric reflectivity profile extended above the surface. The bottom of the beam on the lowest elevation tilt aloft was at a height of 380 meters above ground level (AGL), well above the height of roosting birds, which typically fly at ~50 meters AGL (Larkin, 1991). Clearly, the echo above event # 5 was a rainshower whose degree of asymmetry and stipple was similar from the surface to 2.7 km AGL. Based on these results, stipple could not be used unequivocally to discriminate between birds and weather as the cause for the echoes from 2 June 1990 in Orlando.

41
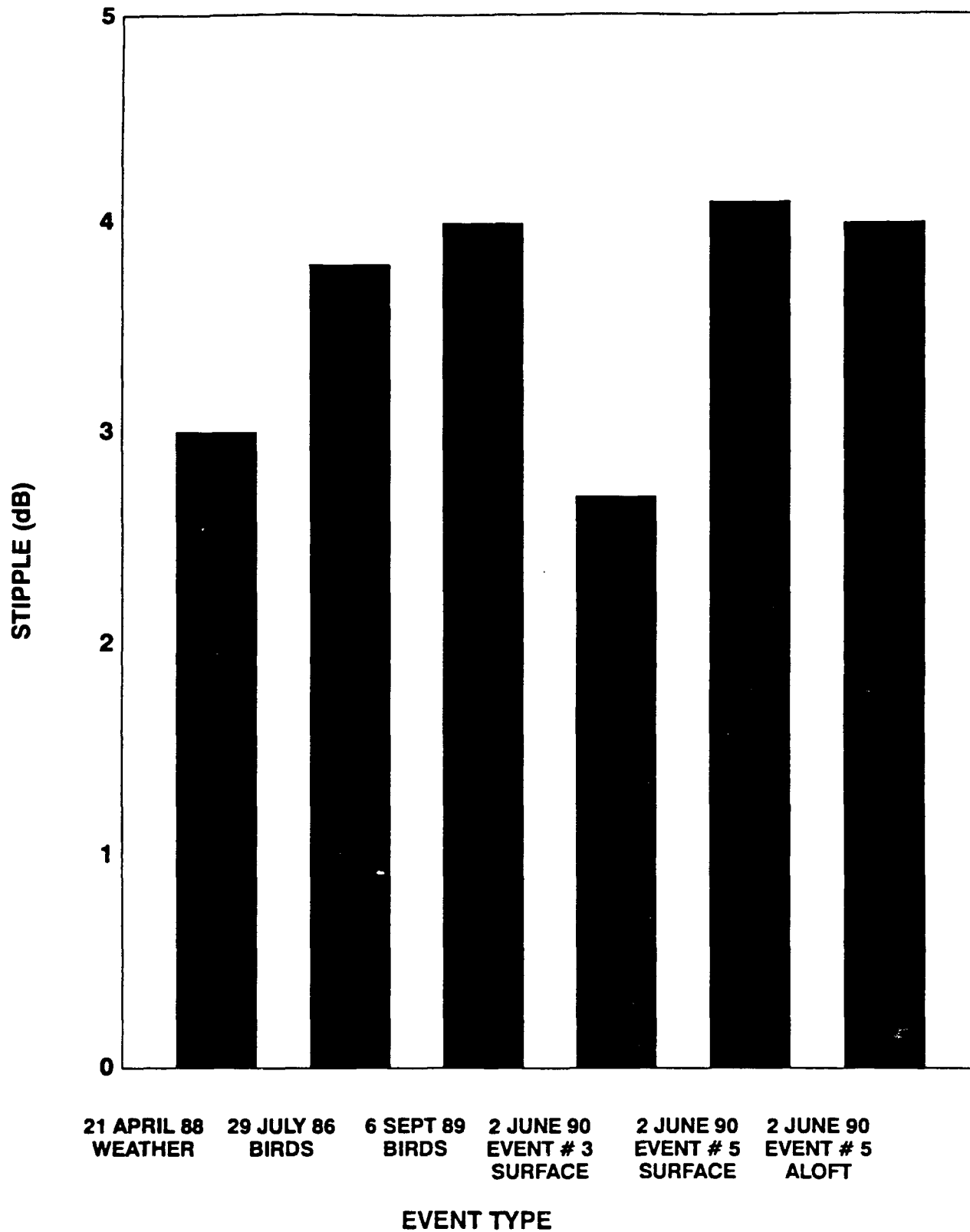
Figure 19. Plot of the average reflectivity stipple for birds, weather, and the 2 June 1990 divergences.

42

6. FEATURES ALOFT

In this section, the vertical structure of the echoes associated with each event will be discussed. As shown in Figure 20., the reflectivity echoes in both cases extended to a height of approximately 10 km AGL. The highest reflectivities were confined to 5 km AGL and below. The maximum reflectivity detected at the surface was similar to the maximum reflectivity aloft in both events.

In terms of the vertical velocity structure, each event was preceded by both mid and upper—level features. The velocity features associated with event # 3 are shown in Table 3. Mid—level rotation first developed at 1831 UT, which is six minutes prior to the initial surface divergence. Both mid—level convergence and upper—level divergence were also detected prior to the event. The maximum velocity differential of the features aloft ranged from 13 to 19 m/s. The height of the rotation at 1837 UT extended from 3.4 to 6.0 km AGL. Mid—level convergence was not as deep, ranging from 4 to 5 km AGL. The velocity features were consistently detected throughout the life cycle of the event.
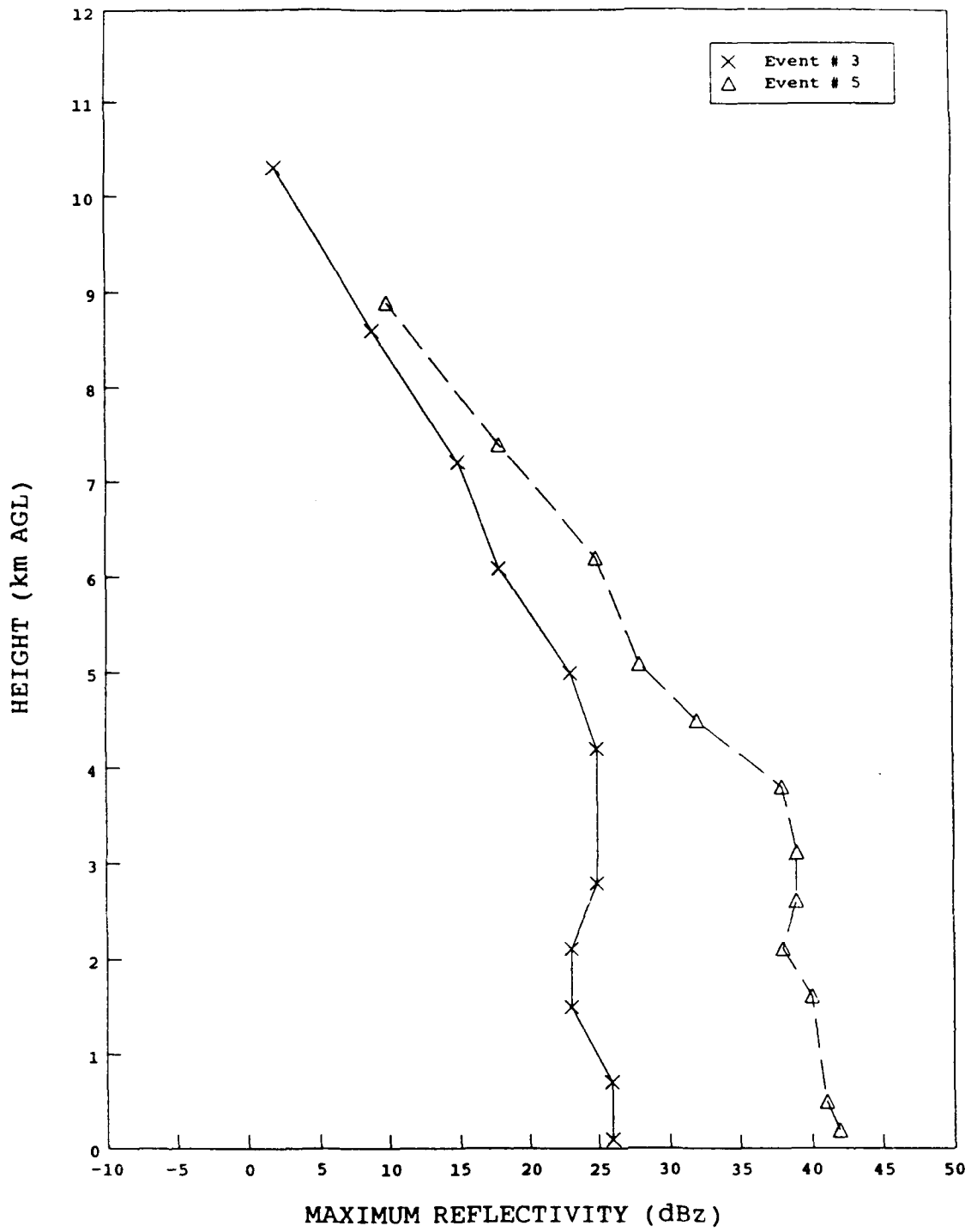
Figure 20. Plot of the vertical profile of maximum reflectivity in events # 3 and 5 vs. height.

44

Table 3.
Characteristics of Velocity Features Aloft with Event # 3
from 2 June 1990 in Orlando, Florida

Time (UT)	Velocity Feature	Delta V (m/s)	Delta R (km) or Delta A (deg)	Height (km AGL)
183108	Cyc. Rotation	15	4.0	3.6
183115	Cyc. Rotation	14	3.5	4.3
183121	Cyc. Rotation	15	3.4	5.1
183121	Convergence	16	1.3	4.9
183243	Divergence	18	1.3	10.3
183402	Anti. Rotation	16	2.4	4.3
183408	Anti. Rotation	16	2.5	5.2
183444	Divergence	19	1.9	10.5
183609	Anti. Rotation	17	3.6	3.4
183615	Anti. Rotation	15	4.2	4.1
183714	Anti. Rotation	14	3.4	6.0
183921	Divergence	18	1.6	7.4
184102	Anti. Rotation	13	3.2	2.9
184109	Anti. Rotation	18	5.1	3.6
184115	Anti. Rotation	15	4.3	4.3
184122	Convergence	18	1.5	4.9
184403	Convergence	13	1.9	4.2
184409	Anti. Rotation	14	3.0	5.0
184621	Anti. Rotation	17	4.5	5.1
184921	Anti. Rotation	14	4.6	4.2

As shown in Table 4., event # 5 was also preceded by mid and upper-level velocity features. Anticyclonic rotation was first detected at 1839 UT, which is 12 minutes prior to the surface divergence. Mid-level convergence and upper-level divergence also developed prior to the event. Both mid-level velocity features (convergence and rotation) were deep, extending from approximately 3 to 6.5 km AGL. The maximum strength of the velocity features aloft varied from 23 to 26 m/s. An example of the convergent signature associated with this event is shown in Figure 21. At 1844 UT, the maximum velocity differential of 18 m/s (+4/−14) is detected over a distance of 1.8 km along an azimuth of 181.5°. By 1847 UT, the velocity differential of the convergence had increased to 22 m/s. The velocity features were consistently detected throughout the life cycle of the event.

Figure 22. shows a vertical velocity and reflectivity image (RHI) of the cell associated with event # 5 at 190015 UT. The maximum reflectivity aloft at this time is only 25 dBz. The highest reflectivities are located near the surface at 13 km range and are somewhat detached from the main echo. The velocity field shows a 20 m/s surface divergence located at a range of 15 km. There is very little velocity structure aloft evident in the RHI. In fact, the mid−level convergence which was detected in the PPI's is not as apparent. The reflectivity structure of this cell is not consistent with other strong microburst−producing storms from Orlando.

PPI Tilt time 06/02/90 18:44:09 to 18:44:13 105 radials Scan 3 Tilt 28 Product v
Spacing = 150m Nyq. vel. = 25.82m/s Unamb. range = 77.7km

RANGE IN KM

PPI Tilt time 06/02/90 18:47:14 to 18:47:18 103 radials Scan 4 Tilt 13 Product v
Spacing = 150m Nyq. vel. = 25.82m/s Unamb. range = 77.7km

RANGE IN KM

Figure 21. BSCAN of the radial velocity of event # 5 at 184409 and 184714 UT.

47
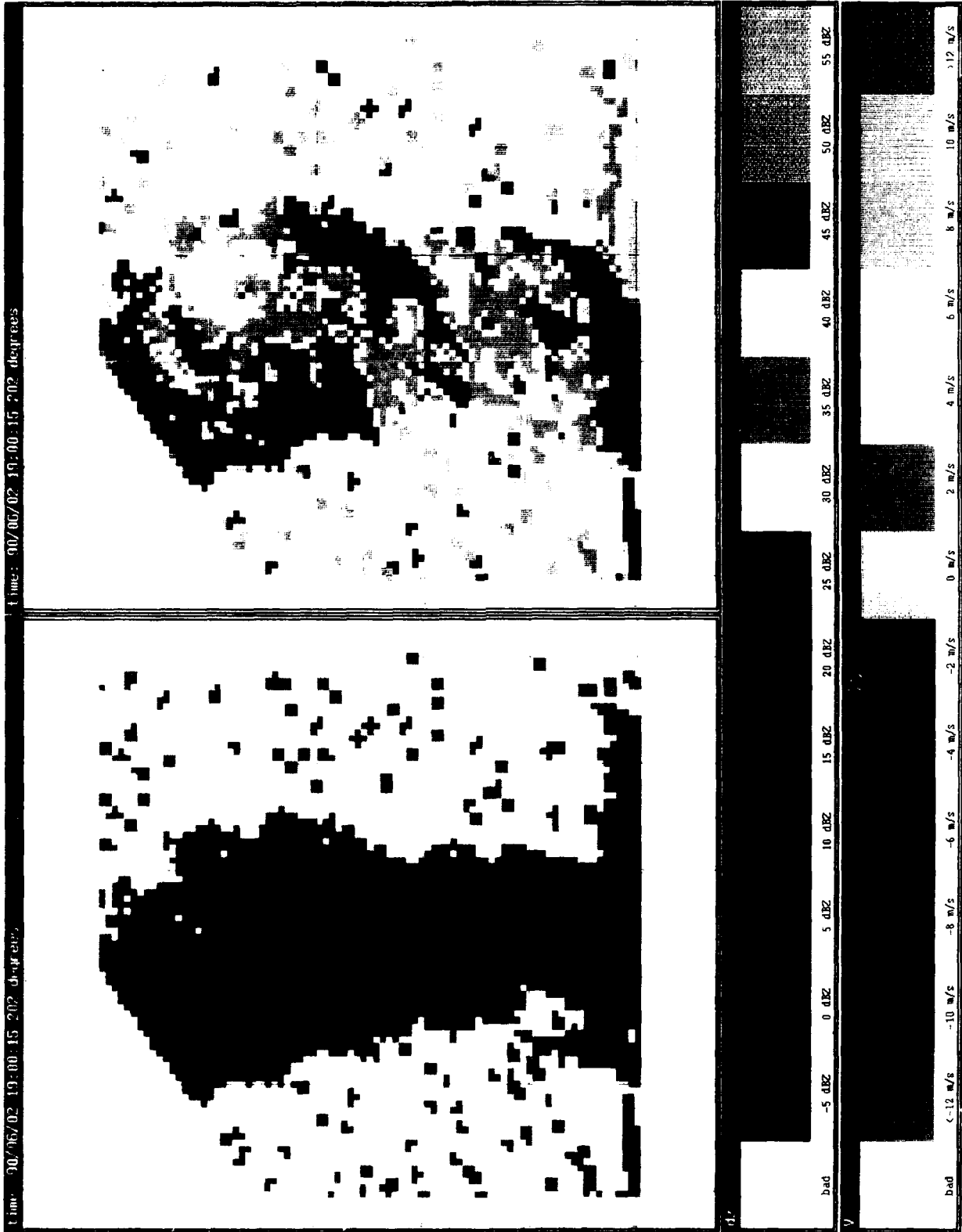
Figure 22. RHI image of the radar reflectivity factor (dBz) and radial velocity (m/s) for event # 5 at 190015 UT on 2 June 1990 in Orlando, Florida. Height (km AGL) is on the vertical axis, while range from the radar (km) is on the horizontal axis.

49

Table 4.
Characteristics of Velocity Features Aloft with Event # 5
from 2 June 1990 in Orlando, Florida

Time (UT)	Velocity Feature	Delta V (m/s)	Delta R (km) or Delta A (deg)	Height (km AGL)
183915	Anti. Rotation	17	5.2	4.6
184237	Divergence	22	1.6	6.7
184403	Convergence	13	1.0	3.3
184409	Convergence	20	0.9	4.0
184415	Convergence	22	1.8	4.9
184431	Divergence	26	1.8	5.9
184438	Divergence	26	2.1	6.9
184712	Convergence	23	1.9	5.0
184720	Anti. Rotation	18	3.0	5.9
184743	Divergence	24	2.7	8.0
184750	Divergence	18	2.7	9.4
184856	Convergence	14	1.5	2.9
184902	Convergence	14	1.7	3.3
184908	Rotation	21	5.8	4.1
184915	Convergence	18	2.4	4.8
184915	Cyc. Rotation	25	4.6	4.9
184921	Cyc. Rotation	22	3.3	5.5
184938	Convergence	20	1.1	6.7
185056	Convergence	11	1.1	1.6
185102	Convergence	12	1.5	2.2
185109	Anti. Rotation	16	2.8	2.8
185115	Convergence	17	1.1	3.3
185115	Anti. Rotation	15	3.3	3.4
185122	Cyc. Rotation	22	4.9	3.9
185214	Cyc. Rotation	22	4.6	4.8
185220	Anti. Rotation	19	3.1	5.6
185237	Divergence	16	1.6	7.2
185243	Divergence	17	1.2	7.9
185323	Anti. Rotation	12	3.2	2.2
185409	Convergence	17	2.0	4.1
185415	Cyc. Rotation	21	4.3	5.1
185415	Convergence	21	2.1	4.9
185421	Cyc. Rotation	22	3.9	5.7

Table 4.
(Continued)

Time (UT)	Velocity Feature	Delta V (m/s)	Delta R (km) or Delta A (deg)	Height (km AGL)
185615	Cyc. Rotation	14	2.9	3.4
185713	Cyc. Rotation	17	5.1	4.6
185743	Divergence	21	2.4	8.1
185908	Convergence	16	2.0	4.0
185914	Anti. Rotation	19	4.0	5.0
190127	Convergence	10	2.1	2.1
190238	Convergence	26	1.7	4.9
190308	Divergence	15	1.2	7.9
190439	Cyc. Rotation	18	3.9	4.1
190651	Convergence	10	2.1	2.0
190711	Anti. Rotation	13	3.9	4.1
190803	Anti. Rotation	17	5.2	4.7
190958	Anti. Rotation	12	3.0	3.9
191004	Anti. Rotation	14	4.5	4.4

7. REFLECTIVITY MEASUREMENTS

In this section, the validity of the reflectivity measurements will be examined. One possible explanation for the low−reflectivity events on this day would be if the radar was not calibrated properly. Between 1989 and 1990, the TDWR testbed was converted from S−band to C−band. The hardware changes required new radar calibration constants. The final parameters were installed by 2 June and there were no subsequent changes to the radar equation in 1990. Therefore, the radar was calibrated prior to the measurements on 2 June.

Another factor which could have contributed to lower reflectivity measurements would be attenuation. This analysis considered both precipitation attenuation along the path and attenuation due to heavy rainfall on the dome. All of the echoes observed on this day were small and generally had low or moderate reflectivities. Throughout the life cycle of event # 3 there was a small 50 dBz echo detected between the radar and the event. The amount of attenuation due to this cell would have been minimal and certainly would not have accounted for the low reflectivity of this echo. There were no echoes detected between the radar and event # 5. At 1905 UT, a small 50 to 55 dBz echo developed over the radar which could have reduced the reflectivity of more distant echoes. However, this could not have accounted for the lower reflectivities recorded in each event prior to this time. The results of this analysis support the conclusion that the reflectivity measurements recorded on this day were valid.

8. ATMOSPHERIC CHARACTERISTICS
FROM CAPE SOUNDING

Besides the radar data which was previously discussed, there is additional evidence to suggest that these divergences were not microbursts. Figure 23. is an atmospheric sounding from Cape Canaveral, Florida at 1015 UT on 2 June. The atmosphere was moist from the surface to approximately 500 mb, with a shallow dry layer at 700 mb. The sounding dries out considerably above the 500 mb level. This is in striking contrast to the typical low–reflectivity microburst sounding from Denver (Wakimoto, 1985) which is characterized by a deep, dry sub–cloud layer with a moist layer aloft. The height of the freezing level was 4.5 km AGL, while the winds were 5 knots or less from the surface to 200 mb. The temperature/dew point spread at the surface prior to the initial divergence was only 7° C (not shown), which is less than half of that documented for low–reflectivity microburst soundings in Denver. The morning sounding
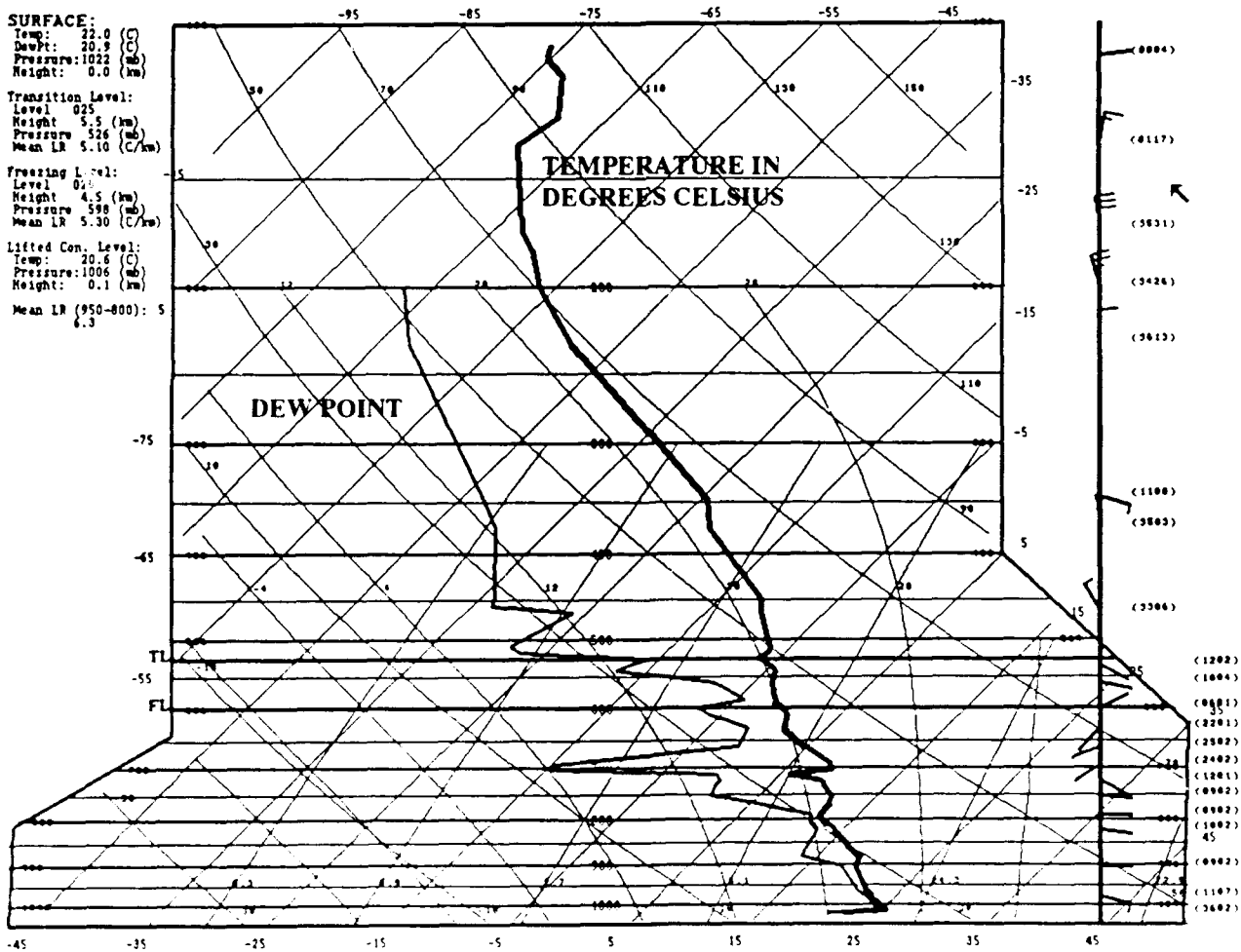
Figure 23. Atmospheric sounding at 1015 UT from Cape Canaveral, Florida on 2 June 1990.

55

from Cape Canaveral does not exhibit any of the characteristics sufficient to produce a strong, low—reflectivity microburst.

Data from the sounding was used to calculate the height of the transition level (level in a moist atmosphere where it changes from conditional or unstable to stable) and the temperature lapse rate from the transition level to the surface. Prior to determining the lapse rate, the sounding was adjusted to account for the pre—event surface temperature and dew point. The upper—air temperatures used to calculate the lapse rate were taken from the sounding. The height of the transition level and the lapse rate will be combined with reflectivity variables such as the precipitation mixing ratio, core depth and core aspect ratio (core depth/core width) to predict the maximum outflow speeds for storms on this day according to the Wolfson Predictive Model (1990). The precipitation mixing ratio was determined by the Marshall—Palmer equation based on the maximum reflectivity. The reflectivity core information was calculated from the dry cell associated with event # 5.

The variables required to predict the maximum outflow speeds are listed in Table 5. The most critical is the lapse rate which, after adjusting for the pre—event surface temperature, was 6.8° C/km. In order for strong outflows to occur at lapse rates below 7° C/km requires a high—reflectivity core (Wolfson, 1988) which was absent in these divergences. Substituting the variables into the Wolfson model resulted in no outflow whatsoever. In order to produce an outflow of 27 m/s would require a lapse rate of 11.5° C/km. A lapse rate of this magnitude would not have been possible on this day, based on the morning sounding from the Cape and pre—event maximum surface temperature. Thus, according to the Wolfson model, these divergences could not have been microbursts unless they were caused by other factors which were not taken into account.

Table 5.
Variables Required to Predict the Maximum Outflow
Speeds on 2 June 1990 in Orlando, Florida

Height of Transition Level (km AGL)	Lapse Rate (°C/km)	Precipitation Mixing Ratio (g/Kg)	Core Depth (km)	Core Aspect Ratio (km/km)
5.5	6.8	0.79	3.1	1.12

9. POSSIBLE MICROBURST FORCING MECHANISMS

In this section, possible microburst forcing mechanisms will be discussed. According to Roberts and Wilson (1988), the primary downdraft forcing mechanisms are evaporative cooling, melting cooling, precipitation drag and vertical pressure gradients. In order for evaporative cooling to occur generally requires either radial convergence below or above cloud base, depending on the moisture profile. For the melting process to force the downdraft depends on radial convergence just below the freezing layer. Precipitation drag requires radial convergence into a descending high−reflectivity core, while the vertical pressure gradient process relies on rotation at low levels. In addition, the strength of the outflow can be influenced by the entrainment of drier air at mid−levels (Roberts and Wilson, 1984), the existence of an elevated stable layer or inversion (Knupp, 1987), or the presence of a newly created pool of slightly cooler outflow air at the surface (Wolfson, 1990).

The importance of precipitation loading was minimal for all of the 2 June low−reflectivity events due to the lack of any well−defined reflectivity core. The process of sub−cloud evaporation relies on a deep, dry sub−cloud layer with a large surface temperature/dew point depression. The morning sounding from the Cape, however, revealed a moist sub−cloud layer with a pre−event temperature/dew point spread much below that documented for low−reflectivity microbursts. The presence of moisture at low levels would inhibit the evaporation process. In order for the vertical pressure gradient theory to apply requires rotation at low levels in the downdraft. While there was rotation with each divergence, it was generally detected at mid levels. Since there was dry air at mid levels, the process of dry air entrainment could not be ruled out. However, its importance is primarily confined to the descent of high−reflectivity cores (Wolfson, 1988). These events certainly do not fit into this category. Melting below cloud base was ruled out since Roberts and Wilson (1984) found this process was restricted to the larger, hail−generating storms. Mid−level convergence preceded each surface divergence; however, the forcing due to evaporation or melting would have been minimal due to the abundant low−level moisture and lack of a descending reflectivity core. Based on these theories for microburst formation, there is no apparent forcing mechanism which could have produced low−reflectivity microbursts on this day.

10. SUMMARY

This report has focused on an analysis of the cause for two low−reflectivity strong divergences which were detected by the TDWR testbed radar on 2 June 1990 in Orlando, Florida. First, the data from birdbursts in Huntsville, Kansas City and Orlando were used to identify candidate features to characterize the phenomena. This analysis showed that there is significant variability in reflectivity, velocity, size and duration of the events, depending on the type and number of birds. This variability makes it difficult to formulate a rule−set for distinguishing bird echoes on radar. Nevertheless, there were distinct patterns in some bird echoes which differentiated them from weather. The best method of discriminating birds from weather in the past was the lack of a reflectivity echo aloft. Another common pattern was caused by large variations over short intervals in the reflectivity or velocity profile. An echo with a low−reflectivity notch in the center which expands outward with time from a fixed location also appears to be a good indication of birds.

Next, the characteristics of the eleven divergences from 2 June were briefly reported. It was shown that the velocity, reflectivity, and duration of these events were similar to the previously studied birdbursts. The most intriguing characteristics were 1) the maximum reflectivity in most cases was less than the typical low−reflectivity microbursts in Denver and 2) four of the divergences were not accompanied by an echo aloft.

An analysis of the reflectivity, velocity and spectral width profiles of two divergences with an echo above the surface followed. Both velocity and spectral width could not be used to determine the cause for either surface divergence. However, the horizontal surface reflectivity profile showed a number of characteristics which were not consistent with weather. For one, the reflectivity distributions were mostly asymmetrical, with the highest reflectivity located within the first few range gates of the signature. By comparison, the horizontal surface reflectivity profiles of weather were more symmetrical. In addition, event # 5 showed a characteristic where the maximum reflectivity and velocity were co−located with a low−reflectivity notch between the peaks, which was similar to the Huntsville Birdburst.

The results of the reflectivity stipple comparison showed that there was little difference in the average stipple between weather, roosting birds, and the two divergences from 2 June. Therefore, stipple could not be used to determine the cause for these divergences.

Finally, the atmospheric characteristics and possible forcing mechanisms were discussed. In order to produce a low−reflectivity microburst generally requires a deep, dry sub−cloud layer, a large temperature/dew point spread at the surface, a moist layer at mid−levels, and a dry adiabatic lapse rate. None of these were prevalent on the pre−event sounding from Cape Canaveral, Florida. In fact, the temperature/dew point spread at the surface was only 7° C, which is half of that documented for low−reflectivity microbursts. According to the Wolfson Microburst Prediction Model, the atmospheric and reflectivity variables from this day would have produced no outflow whatsoever. Based on the low lapse rate, a strong outflow could be

11. CONCLUSION

Based on the sounding data in combination with the reflectivity profiles, we conclude that both low-reflectivity surface divergences examined in this report were caused by the departure of large flocks of birds scattering to avoid a rainshower. It is not unusual to see individual birds or even flocks disturbed from their habitat by rain. The primary basis for this conclusion is that the atmosphere did not contain the temperature or moisture profile sufficient to produce a strong, low-reflectivity outflow. The maximum reflectivity of the events was only 29 and 42 dBz. The high sub-cloud moisture content would rule out the possibility of low-reflectivity microbursts in the Orlando area.

In addition, there were several features in the reflectivity data which were not consistent with weather. For one, the horizontal distribution of surface reflectivity in events # 3 and 5 was highly asymmetrical, with the maximum reflectivity skewed toward the edge of the echo. This type of echo is usually encountered when the environmental winds are strong, which was not applicable in this case. The winds were generally < 5 knots below the transition level. While this skewing of reflectivity may occur in a weather echo, the location of the maximum reflectivity in the first few range gates of the signature was certainly not typical of weather. The co-location of the maximum reflectivity and velocity in event # 5 was also indicative of a bird echo.

Based on the conclusions in this report, the storm cell validation test used in the microburst algorithm did a good job of eliminating potential false alarms. This research has shown the discrimination of birds from weather was hampered by the fact that the bird echoes were co-located with weather echoes. Whenever this happens it will present quite a challenge to the microburst algorithm, especially if a storm cell has been identified nearby. It may be necessary to determine additional methods for discriminating bird echoes in the presence of higher reflectivity weather. Microburst prediction models such as the one developed by Wolfson (1990) may be used to eliminate strong divergences if the atmosphere and reflectivity core information do not support an outflow.

12. FUTURE WORK

In this report, two low–reflectivity surface divergences in Orlando, Florida, were analyzed with radar and atmospheric sounding data to determine what caused each event. It appears the best explanation for these divergences is that they were produced by birds. However, this hypothesis could be conclusively determined only by field verification of the events. Therefore, future work will focus on simultaneous radar and field measurements of birdbursts in central Florida. The high number of lakes and large wintering population of birds in the Orlando area makes this a suitable location for such a study. Field measurements will not only verify the cause for the divergence but also help to determine the type and number of birds. The radar measurements will be compared with data compiled from previous birdbursts to determine if there is a set of features which can reliably discriminate between birds and microbursts, especially if the birdburst is co–located with a weather echo.

13. LIST OF ABBREVIATIONS

AGL   Above Ground Level.

BSCAN   A BSCAN is composed of the radial velocity (m/s) versus range on the horizontal axis and azimuth or elevation on the vertical axis.

C   Celsius.

DBZ   Radar reflectivity factor.

DELTA A   Azimuthal differential in degrees associated with a rotational couplet.

DELTA R   Range difference across the maximum approaching and maximum receding velocities in a convergent or divergent feature.

DELTA V   Radial velocity differential across minimum and maximum velocities in a convergent or divergent feature.

DV/DR   Shear across the divergence/convergence in m/s per kilometer.

KM   Kilometers.

KNOTS   Nautical miles per hour.

MB   Millibars of pressure.

M/S   Meters/second.

NEXRAD   Next Generation Weather Radar.

PPI   Horizontal scan mode.

RHI   Vertical scan mode.

TDWR   Terminal Doppler Weather Radar.

UND   University of North Dakota C−band Doppler weather radar

UT   Universal Time.

14. REFERENCES

F. Caracena and J.A. Flueck, "Forecasting and classifying dry microburst activity in the Denver area subjectively and objectively," *J. Aircraft,* Vol. 25, 525–530 (1988).

J.E. Evans, "Results of the Kansas City 1989 terminal doppler weather radar (TDWR) operational evaluation testing," MIT Lincoln Laboratory, Lexington, Mass., Project Report ATC–171 (1990).

E.H. Houghton, "Detection, recognition and identification of birds on radar," 1964 World Conference on Radio Meteorology, 11th Weather Radar Conference, Boulder, Colorado, 14–21, (1964).

C.J. Kessinger, R.D. Roberts, and K.L. Elmore, "A summary of microburst characteristics from low–reflectivity storms," 23d Conference on Radar Meteorology, Snowmass, Colorado, 105–108, (1986).

K.R. Knupp, "Downdrafts within high plains cumulonimbi, part 1, general kinematic structure," *J. Atmos. Sci.,* 44, 987–1008, (1987).

R.P. Larkin and D.B. Quine, "Draft report on bird movement data," Illinois Natural History Survey, Section on Wildlife Research, University of Illinois, Champaign, Illinois (1987).

R.P. Larkin and D.B. Quine, "Report on bird hazard algorithm," Illinois Natural History Survey, Section on Wildlife Research, University of Illinois, Champaign, Illinois (1989).

R.P. Larkin, "Sensitivity of NEXRAD algorithms to echoes from birds and insects," 25th Conference on Radar Meteorology, Paris, France, 203–205 (1991).

M.W. Merritt, "Microburst divergence detection for terminal doppler weather radar," 24th Conference on Radar Meteorology, Tallahassee, Florida, 220–223 (1989).

M.W. Merritt, D. Klingle–Wilson, and S.D. Campbell, "Wind shear detection with pencil–beam radars," *The Lincoln Laboratory Journal,* Vol. 2, No. 3, 483–510 (1989).

R.E. Rinehart, (personal communication, August 5, 1990).

R.D. Roberts and J.W. Wilson, "Precipitation and kinematic structure of microburst–producing storms," 22d Conference on Radar Meteorology, Zurich, Switzerland, 71–76 (1984).

R.D. Roberts and J.W. Wilson, "A proposed microburst nowcasting procedure using single–Doppler radar," *J. Appl. Met.,* Vol. 28, 285–303 (1988).

W.B. Scott, "Bird Strike suspected as cause of B1–B crash that killed three," *Aviation Week and Space Technology.,* Vol. 21, (1987).

R.M. Wakimoto, "Forecasting dry microburst activity over the high plains," *Mon. Wea. Rev.,* 113, 1131–1143 (1985).

M.M. Wolfson, "Characteristics of microbursts in the continental United States," *The Lincoln Laboratory Journal,* Vol. 1, No. 1, 49–74 (1988).

M.M. Wolfson, "Understanding and predicting microbursts," 16th Conference on Severe Local Storms, Kananaskis Provincial Park, Alberta, Canada (1990).